

TESTING MODELS OF SUPERMASSIVE BLACK HOLE SEED FORMATION THROUGH GRAVITY WAVES

SAVVAS M. KOUSHIAPPAS,^{1,2} ANDREW R. ZENTNER,³

The Astrophysical Journal, submitted

ABSTRACT

We study the gravitational wave background produced from the formation and assembly of supermassive black holes within the cosmological paradigm of hierarchical structure formation. In particular, we focus on a supermassive black hole formation scenario in which the present-day population of supermassive black holes is built from high-mass seed black holes and we compute the concomitant spectrum of gravitational radiation produced by mergers of the seed black holes. We find that this scenario predicts a large, gravitational wave background that should be resolved into individual sources with space interferometers such as the proposed *Laser Interferometric Space Antenna* (LISA). The number of inspiral, merger and ringdown events above a signal to noise ratio of 5 that result from massive black hole seeds is of order 10^3 . This prediction is robust and insensitive to several of the details of the model. We conclude that an interferometer such as LISA will be able to effectively rule out or confirm a class of models where supermassive black holes grow from high-mass seed black holes and may be able to place strong limits on the role of mergers as a channel for supermassive black hole growth. Supermassive black hole seeds likely form in the earliest proto-galactic structures at high redshift and the masses of supermassive black holes are known to be strongly correlated with the potentials of the spheroids in which they reside, therefore these results imply that space interferometers can be used as a powerful probe of the physics of galaxy formation and proto-galaxy formation at very high redshift.

Subject headings: cosmology: theory — dark matter — galaxies: halos — formation — quasars: general — black hole physics

1. INTRODUCTION

The existence of supermassive black holes (SBHs) in the centers of galaxies has been the subject of numerous recent studies. Stellar and gas-dynamical measurements in nearby galaxies and reverberation mapping on high-redshift active galactic nuclei (AGN) have shown that SBHs with masses $M_{\text{BH}} \sim 10^6 - 10^9 M_{\odot}$ reside in the centers of spheroidal systems, these being elliptical galaxies and the bulges of spiral galaxies (for a review, see Ferrarese & Ford 2005). The inferred black hole masses together with measurements of the absolute luminosity of the host spheroids, have revealed a correlation between the mass of the central supermassive black hole, M_{BH} , and the mass of its host spheroid M_{S} (Kormendy & Richstone 1995; Magorrian et al. 1998; Merritt & Ferrarese 2001a). Similarly, detailed studies of the stellar velocity dispersions σ_{*} , in the host spheroids have revealed an even tighter correlation with the mass of the black hole that it is harboring (Ferrarese & Merritt 2000; Merritt & Ferrarese 2001b; Tremaine et al. 2002; Gebhardt et al. 2000). The black hole (BH) and the host spheroid “know” of the presence of one another, though the explanation(s) of this correlation is(are) unknown.

Models of SBH formation and growth should address the following questions.

1. When and where do supermassive black holes, and/or the *seed* black holes from which they grow, form?
2. How do these black holes evolve to the masses that we observe in the local universe?
3. What is the fundamental coupling that connects the stellar dynamics of the bulge to the central black hole?
4. What testable predictions can be used to falsify the model?

In this paper, we show how gravitational wave detectors can be used to test models of seed BH formation. Models in which SBHs form from high-mass ($M_{\text{BH}} \gg 10^3 M_{\odot}$) seeds can be tested explicitly with upcoming gravity wave experiments. As a particular example, we show that the SBH seed formation scenario proposed by Koushiappas et al. (2004, henceforth KBD) makes the robust prediction of a large gravity wave background that should be measurable with a space interferometer, such as the *Laser Interferometric Space Antenna* (LISA)⁴, now in its formulation stage and planned for launch in 2015.

¹ Department of Physics, ETH-Zürich, CH-8093 Zürich, Switzerland

² T-6 Theoretical Division & ISR-1 ISR Division, The University of California, Los Alamos National Laboratory, NM 87545, USA; smkoush@lanl.gov

³ Kavli Institute for Cosmological Physics and Department of Astronomy and Astrophysics, The University of Chicago, Chicago, IL 60637, USA; zentner@kicp.uchicago.edu

⁴ <http://lisa.nasa.gov/>

This is a result with interesting consequences. It provides a method for falsifying models with high-mass black holes seeds, such as the KBD model, for studying the parameters of the KBD-like models, for assessing the importance of mergers in the formation of SBHs, and the establishment of the observed correlations between SBHs and their host spheroids. As we elaborate on below, an important implication then is that LISA can be used as a tool to study the physics of galaxy formation. Moreover, if it were realized in Nature, the gravity wave background that we compute, would represent a significant background contaminant to instruments like LISA and any others that are envisaged for operation in the low-frequency regime, such as the Decihertz Interferometer Gravitational Wave Observatory (DECIGO, Seto et al. 2001) or the Big Bang Observer (BBO)⁵, which could otherwise aim at measuring gravity wave backgrounds arising from the epoch of inflation (e.g. Turner 1997), as a consequence of theories with large extra dimensions (Hogan 2000), or from supernovae (Buonanno et al. 2005).

Numerous scenarios have been proposed for the formation of SBHs. These models address the first three of the above questions through the dynamical evolution of a stellar system (e.g., Quinlan & Shapiro 1990; Hills & Bender 1995; Lee 1995; Ebisuzaki et al. 2001; Miralda-Escudé & Kollmeier 2003; Adams et al. 2003, 2001) or through the hydrodynamical evolution of a pressure-supported object (e.g., Haehnelt & Rees 1993; Loeb & Rasio 1994; Eisenstein & Loeb 1995; Haehnelt et al. 1998; Gnedin 2001; Bromm & Loeb 2003; Koushiappas et al. 2004). In particular, Madau & Rees (2001) (MR01 hereafter) proposed a model where the seeds of SBHs formed at $z \sim 20$ in rare halos ($\sim 3\sigma$ peaks in the smoothed density field) that are sufficiently massive that molecular hydrogen cooling allows runaway collapse of a significant amount of baryons. These baryons form a pressure-supported object of mass $\sim 260M_{\odot}$ that is unstable and collapses to a BH on a timescale of $\sim [1 - 10]$ Myr. Seed BHs in this model have a typical mass $M_{\text{BH}} \sim [1 - 2] \times 10^2 M_{\odot}$. This model is motivated by numerical studies that simulate an extremely dense environment at high-redshift in an attempt to identify the time and environment where the very first luminous objects in the universe form (Abel et al. 2000; Bromm et al. 2001) and evolve (Fryer et al. 2001; Barafee et al. 2001; Heger & Woosley 2002; Shapiro & Shibata 2002; Shaerer 2002). The ramifications of such a scenario were investigated in detail by Volonteri et al. (2003) who demonstrated that subsequent mergers experienced by seed BHs during the formation of a galactic halo do not play a significant role in the growth of the SBH. Instead, a finely-tuned accretion mechanism ensures that SBHs grow in such a way that the relationship between M_{BH} and σ_* is preserved.

Alternatively, KBD proposed a model where seed BHs form from the low angular momentum material in proto-galactic disks at high redshift. This model predicts seed BHs of a specific mass scale, $M_{\text{BH}} \sim \text{a few} \times 10^3 M_{\odot}$ that reside in rare, massive halos at high redshift ($z \gtrsim 12$). BH growth via mergers is more important in this scenario and KBD demonstrated that the slope of the relationship between M_{BH} and M_{S} can be set by hierarchical merging, while the normalization of this relationship may be due to an accretion epoch at some lower redshift. Additionally, KBD showed that if central BHs and their host spheroids are built by mergers, galaxies that do not contain BHs, will also be bulge-less. The transition is set at approximately $M_{\text{S}} \sim \text{few} \times 10^9$ and $M_{\text{BH}} \sim 10^5$, and naturally explains the observational indication of a lower limit on M_{BH} .

Unfortunately, it is difficult to predict robustly observational signatures that can constrain or distinguish between SBH formation scenarios. SBHs may be assembled primarily through mergers of numerous small BHs or relatively fewer mergers of massive BHs. It may be the case that SBHs are formed through periods of possibly super-Eddington accretion (Kawaguchi et al. 2004). One promising avenue for shedding light on the SBH formation mystery is the possible detection of the gravitational waves emitted from mergers during their hierarchical assembly (Thorne & Braginsky 1976). A space-based, interferometric gravity wave detector, such as the proposed LISA interferometer, should be capable of detecting such merger events (Thorne 1995, 1996; Flanagan & Hughes 1998a,b; Cornish & Larson 2001). For such an instrument, mergers of BHs with masses $M_{\text{BH}} \gtrsim 10^3 M_{\odot}$ at redshifts from $z \sim 0 - 30$ will be observable as strain perturbations, providing a new test of the viability of SBH growth through mergers.

The relative importance of mergers and accretion in the growth of SBHs is still under debate. Even if accretion is the dominant growth mechanism, as suggested by studies aiming at explaining the quasar luminosity function (Granato et al. 2001; Salucci et al. 1999; Steed & Weinberg 2003; Haiman & Menou 2000; Hatziminaoglou et al. 2003) and the effect of feedback in the central regions of galaxies and clusters (Pizzolato & Soker 2004; Murray et al. 2005; Dekel & Birnboim 2004; Sazonov et al. 2004), the paradigm of hierarchical structure formation predicts that some growth must be due to mergers. In fact, it may be likely that mergers act as triggers for significant accretion (Armitage & Natarajan 2002; Di Matteo et al. 2005; Springel et al. 2004). Therefore, growth via mergers and accretion may be closely related. A detection of the gravitational wave background due to SBH mergers will directly address the frequency of SBH mergers as well as the BH masses involved in the mergers and hence constrain the relative importance of these events in galaxy formation.

The key ingredients needed to calculate the consequences of hierarchical merging of seed BHs for LISA are the merger rate of BHs as a function of redshift and the distribution of BH masses involved in any particular merger event. Wyithe & Loeb (2003) calculated the merger rate using the extended Press-Schechter (EPS) approximation (Bond et al. 1991; Lacey & Cole 1993) convolved with the empirically-derived relationship between M_{BH} and the velocity dispersion of the host halo. In a similar approach, Rhook & Wyithe (2005) derived a prescription for the black hole occupation distribution and showed that ringdown events will be observed in future gravitational wave detectors. Menou et al. (2001) demonstrated how sensitive gravitational wave detection is to the merger rate of black holes. Another approach was taken in the studies of Sesana et al. (2004a,b) and Islam et al. (2004a,b,c), who populated halos with BHs according to a model like that of MR01 and followed the merger histories of these using the EPS formalism. Enoki et al. (2004) adopted a different method, incorporating BH formation and evolution into a more elaborate, semi-analytic model of galaxy formation (Enoki et al. 2003). Another method for estimating merger rates was proposed by Haehnelt (1994), who developed phenomenological models for mergers based on the number counts of quasars and spheroids. Matsubayashi et al. (2004) showed that different BH assembly scenarios could yield different gravitational wave signatures with calculations based on the runaway SBH

⁵ <http://universe.nasa.gov/program/bbo.html>

formation scenario of Ebisuzaki et al. (2001).

We present estimates of the merger rates and concomitant gravitational wave spectrum in a manner that is qualitatively similar to, but quantitatively different from the approach followed by Sesana et al. (2004a) and Sesana et al. (2004b). We study the consequences of the KBD model of SBH formation which is markedly different from the MR01-type models. As we discuss in detail below, a basic prediction of the KBD model is a characteristic seed BH mass of order $M_{\text{BH}} \sim 10^5 h^{-1} M_{\odot}$, from which larger BHs must be built by mergers and/or accretion (as opposed to $M_{\text{BH}} \sim 10^2 h^{-1} M_{\odot}$ in the MR01-motivated models). The strain induced during a merger event increases with the masses of the merging BHs while the characteristic frequencies decrease with BH mass (precise dependencies depend on the phase of the merger (see for example Flanagan & Hughes 1998a)). It seems reasonable then, that these scenarios result in distinct gravity wave signals. We make specific estimates of BH merger rates by populating halos at high redshift with BHs according to the KBD prescription and we model subsequent dynamics using an approximate, semi-analytic formulation presented by Zentner & Bullock (2003) and expanded upon and tested against a suite of N -body simulations by Zentner et al. (2005). We show that a robust prediction of the KBD scenario is a large gravity wave background. The typical energy density per logarithmic frequency interval, in units of the critical density of the universe ρ_c , has a peak value of $\Omega_{\text{gw}}(f) \sim 10^{-7}$, which is achieved at frequencies $f \sim 10^{-4} - 10^{-2} \text{s}^{-1}$, in an ideal range for the LISA interferometer.

The outline of this manuscript is as follows. In § 2, we provide a brief outline of the KBD model of seed BH formation. In § 3, we step through our algorithm for estimating BH merger rates and present several illustrative, intermediate results that are useful for understanding the typical gravity wave signals. In § 4, we briefly review the emission of gravitational waves by black hole mergers and present our calculation of the cosmological gravity wave background due to mergers of KBD seed BHs. We present our results in § 5. We summarize our results and present our conclusions in § 6.

We perform all of our calculations in the context of a standard, flat Λ CDM cosmology with $\Omega_M = 0.3$, $\Omega_{\Lambda} = 0.7$, $h = 0.7$ and a power spectrum normalization of $\sigma_8 = 0.9$ (Tegmark et al. 2004). In what follows, we use the specifications of the proposed LISA instrument as an example of a gravity wave detector operating in the low-frequency regime.

2. THE FORMATION OF SUPERMASSIVE BLACK HOLE SEEDS

In the scenario for SBH assembly proposed by KBD, BH seeds form from the lowest-angular momentum baryonic material in proto-galactic disks. Unlike the model of Eisenstein & Loeb (1995), where seed BHs are formed in the centers of dark matter halos with low *net* angular momentum, KBD proposed that seed BHs form from the lowest-angular momentum material in all halos that are able to assemble self-gravitating disks. Here, we give a brief overview of this mechanism for the generation of seed BHs and refer the reader to Koushiappas et al. (2004) for more details.

In the standard scenario of galaxy formation, galaxies form in halos that are massive enough to trap and cool baryons efficiently (White & Rees 1978). The host dark matter halos acquire their angular momenta through tidal torques induced by neighboring quadrupole fluctuations in the density field. Baryons are assumed to have an angular momentum distribution that mirrors that of dark matter at very high redshift. Both van den Bosch et al. (2002) and Chen et al. (2003) tested this assumption using hydrodynamic cosmological simulations, and found it to be approximately correct. We still lack a detailed understanding of the evolution of the angular momentum distribution of baryons, yet the assumption that gas follows dark matter at high redshift is reasonable.

Unlike the dark matter, baryons are collisional. Once trapped in dark matter potential wells, baryons cool by radiating their kinetic energy and fall further down the potential (e.g. see Tegmark et al. 1997, for a summary). At high temperatures ($T \gtrsim eV$), cooling proceeds via Bremsstrahlung radiation and collisional excitations. Further cooling requires the presence of molecular hydrogen. Halos that cool efficiently are sufficiently massive that the production rate of molecular hydrogen is large enough to induce cooling on a timescale much shorter than a Hubble time. Once baryons begin to cool, they agglomerate at the halo center, and are expected to form a high-density, proto-galactic disk. The surface density of the disk is set by the angular momentum distribution of baryons. We assume an initial angular momentum distribution proposed by Bullock et al. (2001) (B01 hereafter). In halos that efficiently cool their gas, a proto-galactic disk, with a surface density profile set by the B01 distribution, forms within roughly a dynamical timescale. Early on, this disk is pressure-supported. As more mass is added to the disk, the presence of local gravitational instabilities starts to overcome the pressure support. In the inner parts of the disk, where such processes likely occur due to the higher densities, gravitational instabilities manifest themselves as an effective viscosity (Lin & Pringle 1987). This viscosity leads to angular momentum transfer from the inner disk outward. Some material in the inner disk loses angular momentum resulting in the flow of mass to the center. Eventually, instabilities in the disk become fully dynamical and the first generation of stars forms. These first stars are thought to be massive, with lifetimes of order $t_{\text{fs}} \sim 1 - 10 \text{Myr}$ (Barafee et al. 2001; Heger & Woosley 2002; Shapiro & Shibata 2002). The presence of these first stars and their subsequent supernovae explosions likely result in significant heating of the disk. As the temperature of the disk increases, angular momentum transfer ceases to be effective and mass inflow stops. Therefore, once gravitational instabilities become effective, the accumulation of mass at the center of the halo proceeds for a time $\sim t_{\text{fs}}$ and then stops.

The above scenario assumes that the disk forms and evolves uninterrupted over many dynamical times. However, a major merger is likely to disrupt any disk and halt this process prematurely. Thus this process proceeds in halos that are both large enough to cool their gas *and do not experience major mergers*. In practice, the latter criterion proves most stringent. We estimate the major merger timescale as the average time for a halo to double its mass according to the EPS approximation, then we require this timescale to be longer than the time required to go through the above process. This sets the effective lower limit on the mass of halos that may form seed BHs. We depict this *critical mass* $M_{\text{v,crit}}(z)$, for seed BH formation as a function of redshift as the *solid* line in Figure 1. In addition, we show contours in the Mass-redshift plane for $2 - 6\sigma$ fluctuations in the smoothed density field (using a standard top-hat window) to illustrate that this process proceeds in rare halos.

By the time the viscous transport process terminates, a baryonic mass of order $\sim 10^5 h^{-1} M_{\odot}$ is transferred to the center of the super-critical halos. Such an object may be briefly pressure-supported, but it inevitably collapses to form a BH due to the post-Newtonian

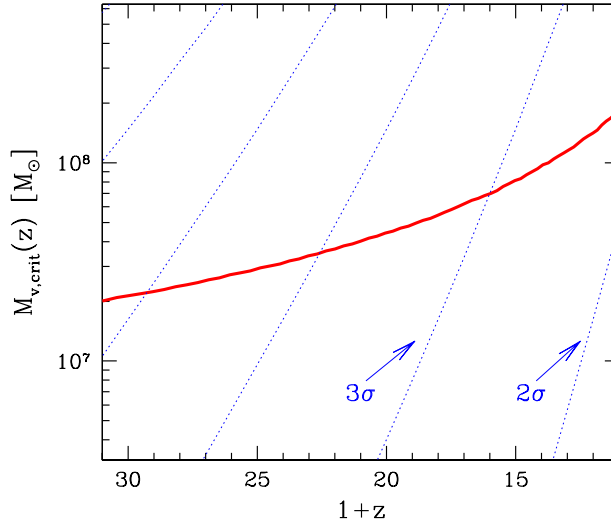


FIG. 1.— The critical mass for seed black hole formation as a function of redshift (solid line) in the KBD model. The dotted lines correspond to 2σ - 7σ fluctuations in the smoothed density field indicating that the critical masses of concern are rare systems.

instability (Shapiro & Teukolsky 1983). In this regard, the KBD model distinguishes itself from models based on the proposal of Madau & Rees (2001). The KBD model predicts a characteristic minimum mass for the first, seed BHs of order $M_{\text{BH}} \sim 10^5 h^{-1} M_{\odot}$. In detail, the distribution of angular momenta exhibited by simulated cold dark matter halos manifests itself as a distribution in the masses of seed BHs formed via the KBD mechanism. Given a host halo mass $M_{\text{vir}} \geq M_{\text{v,crit}}$ at z , the probability that a seed BH of mass M_{BH} is formed within this halo is given by

$$P(M_{\text{BH}})dM_{\text{BH}} = \frac{1}{\sqrt{2\pi}} \frac{1}{\sigma_{M_{\text{BH}}}} \times \exp\left[-\frac{\ln^2(M_{\text{BH}}/M_{\text{BH}}^0)}{2\sigma_{M_{\text{BH}}}^2}\right] dM_{\text{BH}} \quad (1)$$

where M_{BH}^0 is

$$M_{\text{BH}}^0 = 3.8 \times 10^5 M_{\odot} \left(\frac{M_{\text{vir}}}{10^8 M_{\odot}}\right) \left(\frac{f_{\text{cb}}}{0.03}\right)^{3/2} \times \left(\frac{1+z}{18}\right)^{3/2} \left(\frac{t_{\text{fs}}}{10\text{Myr}}\right) \quad (2)$$

and $\sigma_{M_{\text{BH}}} = 0.9$ (Koushiappas et al. 2004). In Equation 1, f_{cb} is the fraction of cold baryons that form the self-gravitating disk in time t_{fs} . This is some fraction of the total possible baryonic material that can cool f_0 , which we take to be roughly $\sim 20\%$ of the universal baryon fraction in a Λ CDM cosmology.

The epoch of cosmological reionization places a lower limit on the redshift at which this process can operate. Heating of the intergalactic medium (IGM) prevents molecular hydrogen production and essentially cuts off the accretion and cooling of baryons in small systems. Thus, any significant IGM heating, such as that associated with reionization, effectively stops KBD BH formation. For simplicity, we assume that seed BH formation stops abruptly and we refer to the redshift at which the KBD scenario effectively terminates as z_{re} ⁶.

In summary, the KBD model contains three key input parameters: the total fraction of mass that can cool via molecular hydrogen, f_0 ; the timescale for the evolution of the first stars, t_{fs} ; and the redshift at which reionization heats the IGM to a degree that this process is no longer effective, z_{re} . Varying these parameters within a reasonable range, the predictions of the KBD model are most sensitive to z_{re} . This can be seen from Figure 1. z_{re} sets the final redshift at which this process is effective and varying this redshift changes the rarity of the halos in which this process can take place. In what follows, we adopt typical, fiducial values of $f_0 = 0.2$ and $t_{\text{fs}} = 10$ Myr and present results for $z_{\text{re}} = 8$, $z_{\text{re}} = 12$ and $z_{\text{re}} = 16$. Lower values of z_{re} lead to more BHs and larger gravity wave signals, while it is interesting to explore high values of z_{re} because they represent a minimum expected signal in this type of scenario and a high z_{re} is supported by the cosmic microwave background anisotropy temperature-polarization cross correlation (Spergel et al. 2003; Page et al. 2003).

⁶ In the context of the KBD model, the inferred mass density of black holes at z_{re} allows for growth via accretion by a factor of ~ 10 in mass, consistent with the growth experienced during an AGN phase of order a Salpeter time in duration. This is in contrast to the model of Volonteri et al. (2003) where in order to reproduce the observed mass density of black holes, the small mass seeds of that model are expected to experience significant accretion after *each* major merger experienced by their host halo.

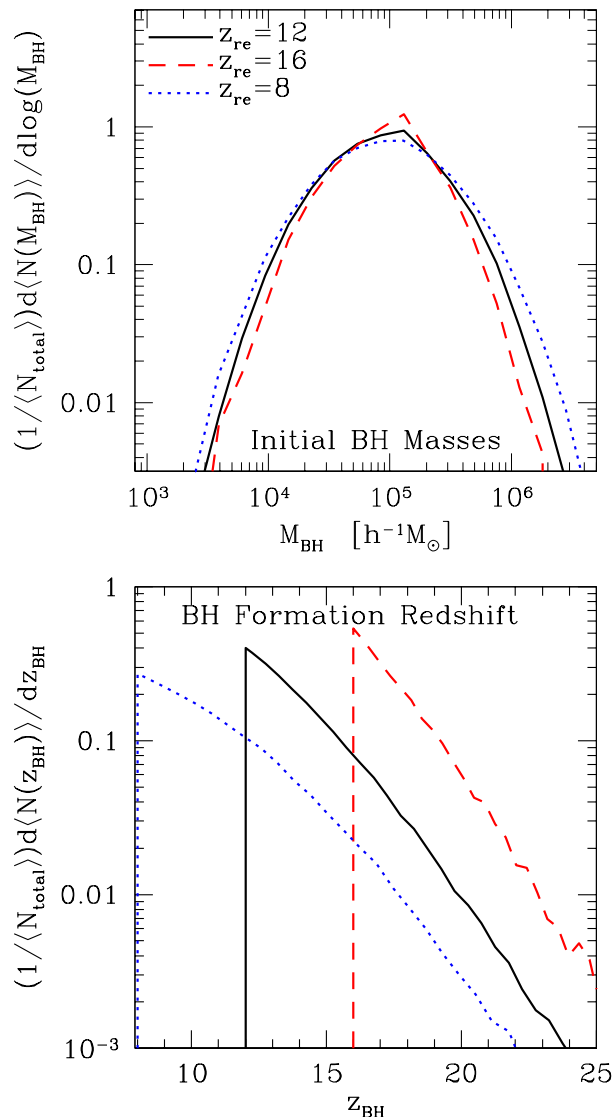


FIG. 2.— *Top*: The initial seed BH mass spectrum. At the top of the panel we show the mean total number of black hole seeds per merger history realization in each case. These numbers provide the normalization for the curves. *Bottom*: The distribution of seed BH formation redshifts. In both panels, *solid* lines correspond to our fiducial case of $z_{\text{re}} = 12$ while *dashed* lines correspond to $z_{\text{re}} = 16$ and *dotted* lines correspond to $z_{\text{re}} = 8$. The sharp cutoffs represent the end of BH seed formation at z_{re} . The results in both panels are from 200 realizations of the formation history of a halo of mass $M_{\text{vir}} = 10^{12.1} h^{-1} M_{\odot}$, which is comparable to the mass of the Milky Way halo.

3. ESTIMATING BLACK HOLE MERGER RATES

In order to compute the gravitational wave signal due to BH mergers, we must compute the merger rate of black holes as a function of redshift and BH mass. We do this in three steps. First, we use the results of the KBD model, described in § 2, to establish a population of seed BHs in host halos at high redshift. Second, we estimate the rate at which BHs pairs are brought into the central region of a common halo center. To compute the rate of formation of these *potential pairs*, we use a semi-analytic model for halo mergers and the dynamical evolution of subhalos within larger host halos. We refer to this as the *halo evolution* stage. These first two ingredients are based on the semi-analytic model of halo substructure evolution presented in Zentner & Bullock (2003) and Zentner et al. (2005). Once potential pairs are formed within a halo, we estimate the timescale over which the BHs move from a separation of order a large fraction of a kpc to a separation close enough to emit gravitational radiation. We refer to this stage as *migration*.

3.1. Populating Halos with Black Hole Seeds

The first step is to establish a primordial population of seed BHs predicted by the KBD model. Consider a halo of virial mass M_{vir} at $z = 0$. We use the extended Press-Schechter formalism (Bond et al. 1991; Lacey & Cole 1993) to compute merger histories, which consists of a list of all of the smaller halos that merged together to form this final halo and the redshifts at which these mergers occurred. This is a Monte Carlo procedure and by repeating the procedure many times for the same host mass, we sample the variety of different accretion histories that lead to a halo of fixed mass at $z = 0$. We refer to each sample merger history that we construct as

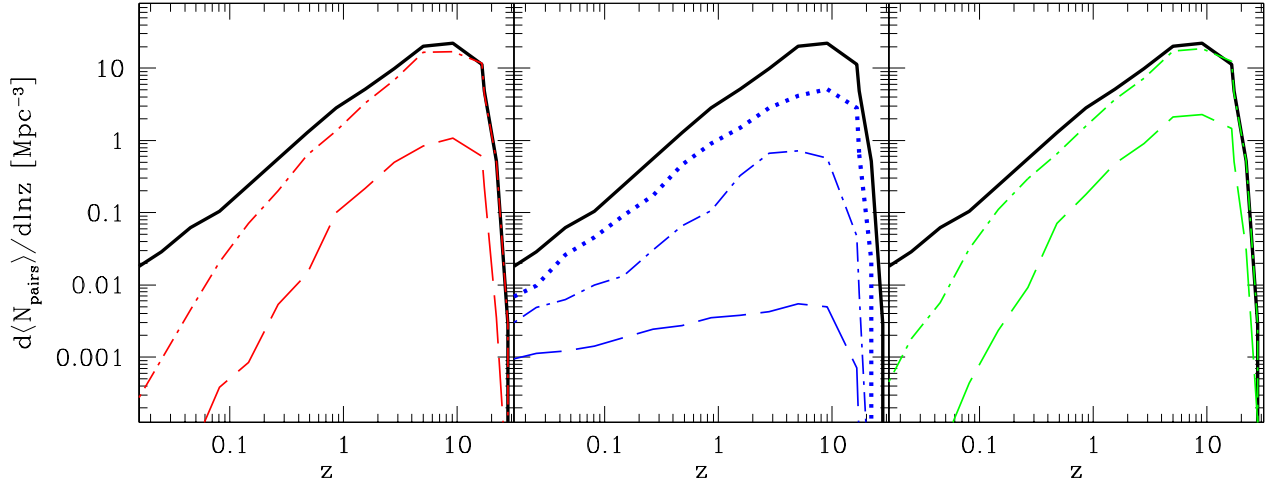


FIG. 3.— The mean comoving number density of potential BH pairs as a function of redshift for the fiducial case of $z_{\text{re}} = 12$. In all three panels, the *thick, solid* curve represents the total number density of potential BH pairs. *Left:* The *dot-dash* line represents the total number density of potential BH pairs for which the total mass in the binary is $M_1 + M_2 \leq 10^6 M_\odot$, while the *dashed* line depicts all pairs with $M_1 + M_2 \leq 10^5 M_\odot$. *Middle:* The *dotted* line represents the number density of pairs where the ratio of black hole masses is $M_2/M_1 \leq 10^{-1}$, the *dot-dashed* line shows the pairs with $M_2/M_1 \leq 10^{-2}$, while the *dashed* line corresponds to pairs with $M_2/M_1 \leq 10^{-3}$. *Right:* Here, the *dot-dashed* line represents pairs where the most massive black hole mass is $M_1 \leq 10^6 M_\odot$, while the *dashed* line depicts pairs where $M_1 \leq 10^5 M_\odot$.

a merger history *realization*. In an individual realization, each merger represents a branch in the *merger tree*. At each branch, each merging halo has its own merger history that we can follow and so on. The resulting merger tree structure describes the ways in which a halo of mass M_{vir} today breaks up into *halos* of various masses as a function of redshift. We use the particular implementation of the EPS formalism advocated in Somerville & Kolatt (1999), to which we refer the reader for further details.

We follow each branch to higher redshift and smaller mass until one of two things happens. If the branch is above $M_{\text{v,crit}}(z)$ at some redshift $z > z_{\text{re}}$, then we find the earliest time in its mass accretion history that the halo mass was greater than $M_{\text{v,crit}}(z)$. At this time we assign this the redshift of BH formation, z_{BH} . We choose the earliest time because we assume that subsequent mergers between super-critical halos do not restart the process described in § 2. This is because once a halo goes through the mechanism of BH formation described in § 2, the presence of metals left over from the first generation of stars in the disk alters the properties of the disk, making it significantly more susceptible to fragmentation. We then assign the halo a BH mass according to the probability distribution in Equation 1. Alternatively, if there is no point on the branch where $M > M_{\text{v,crit}}(z)$ at $z > z_{\text{re}}$, we eliminate this branch from further consideration. In this case, the halo does not meet the conditions necessary for the formation of a SBH seed and can not host a BH.

As an example of the product of this procedure, in Figure 2 we show initial spectra of seed BH masses and formation times. In this specific demonstration, we calculate these quantities by averaging the results of 200 merger histories of halos of final mass $M_{\text{vir}} = 10^{12.1} h^{-1} M_\odot$, comparable to the halo of the Milky Way (Klypin et al. 2002), with our fiducial value of $z_{\text{re}} = 12$, as well as low and high reionization redshift alternatives $z_{\text{re}} = 8$ and $z_{\text{re}} = 16$. The mean total number of seed black holes is $\langle N_{\text{total}} \rangle = 589$ for the fiducial case of $z_{\text{re}} = 12$, while for $z_{\text{re}} = 8$ and $z_{\text{re}} = 16$ this number is $\langle N_{\text{total}} \rangle = 1601$ and $\langle N_{\text{total}} \rangle = 122$ respectively. The spectra in Figure 2 are normalized to the mean number of seed BHs. First, notice that the formation redshifts are peaked at $z_{\text{BH}} = z_{\text{re}}$ in all cases. Figure 1 shows halos that are suitable hosts for BH seeds become increasingly rare as redshift increases with the result that most BHs form at $z \sim z_{\text{re}}$. Additionally, the initial BH mass spectrum is a broad distribution. In our fiducial case, it is roughly log-normal with $\langle \log(M_{\text{BH}}/h^{-1}M_\odot) \rangle \approx 5.4$ and a large dispersion, $\sigma(\log_{10}(M_{\text{BH}})) \approx 0.45$. This mass distribution is broader than that of Eq. 1, due to the variety of different halos and redshifts at which these seed BHs may form. The distribution gets systematically narrower with increasing z_{re} because the halos suitable for seed BH formation become increasingly rare so that BH formation occurs in correspondingly narrower ranges of host halo mass and formation redshift.

3.2. Halo Evolution

With initial BH populations in place, the next step is to compute the evolution of the BHs and their host halos, as they merge. We do this using a semi-analytic model for the merging and evolution of substructure in a larger main halo described in detail by Zentner et al. (2005). In this section, we outline this model.

First, merger trees are constructed as described in § 3.1. Each halo of mass M_{vir} today forms from a sequence of mergers with halos of smaller mass. We refer to the larger of the pair as the *main halo* and the smaller as a *subhalo*. BH mergers are always preceded by these halo mergers as it is the halos that bear the infalling BHs. BHs are brought near the center of the main halo, where they presumably merge, primarily due to dynamical friction acting to remove orbital energy from the orbiting subhalo. Roughly speaking, the deceleration due to dynamical friction is proportional to the bound mass of the subhalo, so the loss of mass due to the tides raised by the potential of the main halo must also be modeled in order to make an estimate of the timescale on which subhalos bring BHs

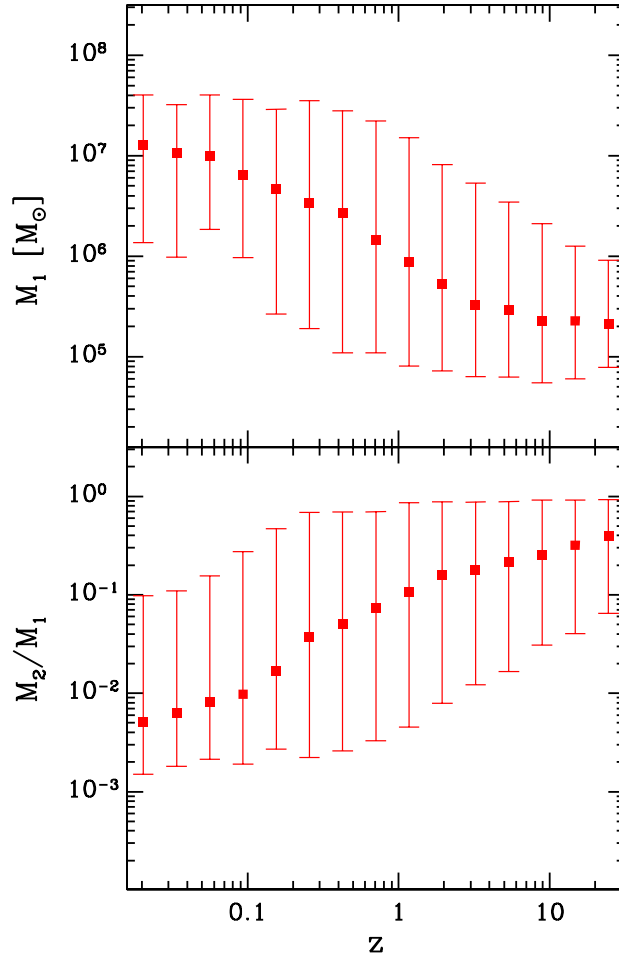


FIG. 4.— *Top*: The median mass of the heaviest BH in a pair as a function of redshift. The error bars represent the 90 percentile range of black hole masses. *Bottom*: The ratio of the lighter to the heavier black hole mass M_2/M_1 , in a pair as a function of redshift. Errorbars are as in the top panel.

to the central regions of the main halo.

We track the evolution of subhalos as they evolve in the growing, main system in the following way. At each merger event, we first assign initial orbital energies and angular momenta to infalling subhalos according to the probability distributions culled from cosmological N -body simulations (Zentner et al. 2005). We then integrate the orbit of the subhalo in the main halo from the time of accretion to the present day. We model tidal mass loss using a modified tidal approximation and dynamical friction using a modified form of the Chandrasekhar formula (Chandrasekhar 1943), as described in detail in Zentner et al. (2005). For simplicity, we model all halos by the density profile of Navarro et al. (1997) (NFW). Zentner et al. (2005) showed that this model is in excellent agreement with the results of direct simulation over several orders of magnitude in halo mass and over a wide range of redshifts. The only modification that we make to the prescriptions in Zentner et al. (2005) is that halos may have an additional point mass representing the BHs at their centers. In practice, the presence of the BHs make little difference in the large-scale dynamics because the BH masses are $\lesssim 10^{-3}M_{\text{subhalo}}$. Subhalos that approach the central \sim few kpc of the main halo lose most of their mass due to tides, yet their BHs continue to orbit the host. Once the apocenter of an orbiting system becomes very small, we cannot continue to track its evolution for two reasons. First, the dynamical timescales in the central halo are quite short so that very small timesteps are needed to integrate the orbit and the calculation becomes unmanageable. Second, our simple model of subhalo evolution is not applicable near the centers of halos where interactions with the central galaxies often dominate interactions with halo potentials. We follow the approach of Islam et al. (2004a) and cease tracking the orbits of all subhalos and BHs that reach an apocentric distance from the center of the main halo that is less than $r_{\text{pp}} = \min(0.01R_{\text{vir}}, 1 \text{ kpc})$, where R_{vir} is the virial radius of the main halo. We refer to the resultant pairs that are separated by $\sim r_{\text{pp}}$ as *BH potential pairs*. In this way, we decouple the large-scale subhalo dynamics that bring the BHs from a separation of $\sim R_{\text{vir}}$ to a distance $\lesssim 0.01R_{\text{vir}}$, from the subsequent processes that determine the rate at which potential pairs evolve into binaries and merge. We discuss this final stage of BH *migration* in the following subsection.

For the purposes of our modeling here, we compute 25 merger tree and subhalo evolution realizations at 15 values of the $z = 0$ host mass M_{vir} , starting at $M_{\text{vir}} = 10^{11} h^{-1}M_{\odot}$ and increasing in steps of $\Delta[\log(M_{\text{vir}})] = 0.25$. We find that extending the computation to smaller masses does not influence our results because smaller halos generally host few BHs, while extending our computation to higher masses does not affect our results because of the relative rarity of such large halos.

We show an example of the intermediate results after this second stage of modeling in Figure 3. In this Figure, we plot the mean comoving number density of black hole pairs as a function of redshift. At high redshift and up to the redshift of reionization there is a linear increase of BH pairs as new seed black holes are being formed (see discussion in Section 2). The increase in potential pairs comes from the fact that halos that are able to host seed black holes become increasingly more abundant with decreasing redshift. At reionization seed BH formation ceases to operate and the number of BH pairs is governed solely by the interplay of halo merger rates and dynamics. The former depend on the underlying cosmological model, while the latter depend on the details of dynamical friction, tidal heating, and mass loss.

Figure 4 depicts the masses of the black holes that form the potential BH pairs. As expected, at early times, prior to significant merger activity, the masses of BHs in the centers of all halos are of the same order as the seed BH masses in Eq. (1). As major mergers bring more BHs to the center, the masses of BHs in large halos increases. Mergers of small, satellite black holes with larger, central BHs that are themselves the products of mergers become more common and drive the ratio M_2/M_1 down with decreasing redshift. The relatively greater importance of these mergers with remnants of previous mergers at low redshifts can also be gleaned from Fig. 3. Again, we emphasize that the number of BHs and BH pairs is sensitive to z_{re} , yet the masses are not because $M_{\text{v,crit}}$, and consequently the typical BH mass M_{BH}^0 varies very slowly with redshift [see Fig. 1 and Eq. (1)].

3.3. Black Hole Migration

As we showed in the previous subsection, we track BHs until the distance between the parent BH and the merging BH is $r_{\text{pp}} = \min(0.01R_{\text{vir}}, 1 \text{ kpc})$. This distance is much larger than the distance where gravitational radiation becomes an important channel for energy loss from the pairs. Somehow, the infalling satellite BHs in the potential pairs must *migrate* to the center. This can be achieved either through stellar interactions (Begelman et al. 1980; Quinlan 1996; Milosavljević & Merritt 2001; Yu 2002), or various gas dynamical effects (Gould & Rix 2000; Armitage & Natarajan 2002; Kazantzidis et al. 2004). Sesana et al. (2004a,b) calculate the timescale for the pair to reach the gravitational radiation regime due to stellar interactions, following the analysis of Quinlan (1996). In order to implement such a scenario, they make the mapping between velocity dispersion and halo circular velocity based on an empirical relationship (Ferrarese 2002). The subsequent hardening of the binary proceeds through the capture and ejection of nearby stars. Such estimates require numerous uncertain assumptions. Instead, we choose to leave the migration timescale t_{mig} as a parameter, and investigate the consequences of various migration timescales on our final results.

We can make very rough estimates of the range of values that t_{mig} may plausibly take. The fastest timescale within which a black hole would be able to migrate to the center of the halo is the dynamical timescale. If we assume black holes are at a distance r_{pp} from the center, then typical values of the dynamical timescale are of order $\sim \text{Myr}$ for the halos that host black holes in our model. Black holes may sink to the center by exchanging their orbital energy with nearby gas, stars and dark matter. If we follow the method of Sesana et al. (2004a,b), we find that the migration timescale ranges from $t_{\text{mig}} \sim 1 \text{ Myr}$ to a few Gyr, depending upon the initial configuration of the pair (r_{pp}), the properties of the host halo (M_{vir}), and the central stellar population. The latter can be obtained given the mass of the host halo and the empirically-derived relationship between stellar velocity dispersion and halo circular velocity (Ferrarese 2002). We assume t_{mig} takes values that range from $t_{\text{mig}} = 1 \text{ Myr}$ to $t_{\text{mig}} = 1 \text{ Gyr}$, to cover a range of reasonable expectations. Migration timescales in excess of a $t_{\text{mig}} \sim 1 \text{ Gyr}$ will most likely be altered by other processes because the major merger timescale is of the same order. In this case, the pair may get disrupted, and/or following a potential 3-body interaction, the characteristics of the pair may change (for a comprehensive review of the evolution of BH binaries see Merritt & Milosavljevic (2004)).

The net effect of changing the value of t_{mig} is easy to understand in general. If we choose the lower bound, $t_{\text{mig}} \sim \text{Myr}$, almost all pairs will reach the gravitational emission regime by $z = 0$. On the other hand, if $t_{\text{mig}} \sim \text{Gyr}$, pairs that are formed at redshifts smaller than $z \lesssim 0.1$ will not reach the gravitational emission regime by today. However, as can be seen in Figure 3, the fraction of mergers occurring at $z \lesssim 1$ is rather small so the effect on the cumulative gravitational wave background is small. Thus, the choice of t_{mig} is *not* crucial to our results.

4. GRAVITATIONAL WAVE EMISSION FROM BLACK HOLE MERGERS

4.1. Gravity Waves From Individual Mergers

In this section, we briefly review the emission of gravitational waves from coalescing BH pairs. Most of our review follows from the comprehensive discussions in Misner et al. (1973), Thorne (1980), Thorne (1987), Flanagan & Hughes (1998a,b), and Cornish & Larson (2001). We refer the reader to these resources for details.

As in electromagnetism, the gravitational radiation field can be decomposed into multipoles and the energy output is typically dominated by the lowest non-vanishing multipole. In the case of electromagnetic radiation, this is usually the dipole, whereas gravity is a tensor field so the lowest non-vanishing term is typically the quadrupole. The power output in quadrupolar radiation from a slowly-moving, weak-field gravity wave source is then similar to the familiar far-field relation for electromagnetic quadrupole radiation (Jackson 1975) and is given by (e.g. Misner et al. 1973)

$$\frac{dE}{dt} = \frac{c^5}{G} \left\langle \frac{d^3 I_{jk}}{dt^3} \frac{d^3 I^{jk}}{dt^3} \right\rangle, \quad (3)$$

where

$$I_{jk} = \int \rho \left(x^j x^k - \frac{1}{3} r^2 \delta_{jk} \right) d^3x \quad (4)$$

is the moment of inertia of the mass distribution and overdots denote time derivatives.

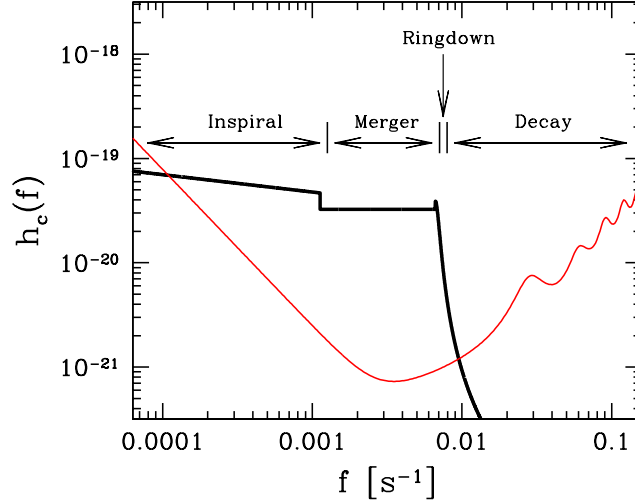


FIG. 5.— An example of the strain induced by a high-redshift black hole merger. The different merger phases in a pair of masses $M_1 = 1.5 \times 10^5 M_\odot$ and $M_2 = 1.1 \times 10^5 M_\odot$ that initiates gravitational wave emission at $z = 13$ (thick line). The 1σ detection threshold for burst sources with LISA is shown as the thin curve (e.g. Thorne 1987, 1996; Larson et al. 2001).

Rather than flux, gravity wave detectors measure the wave amplitude through the fractional change in the physical separation of two masses, expressed as the strain $h(t)$. The metric perturbation due to the wave $h_{\mu\nu}(t)$, contains two polarizations, which in the transverse-traceless gauge, are conventionally labeled as $h_+(t)$ and $h_\times(t)$. If we define the Fourier transform of $h_i(t)$, with $i = +, \times$, as $\tilde{h}_i(f) = \int_{-\infty}^{+\infty} h_i(t) e^{2\pi i f t} dt$, then the one-sided spectral density of gravity waves $S_h(f)$ is defined as $2 \sum_i \langle \tilde{h}_i^*(f) \tilde{h}_i(f') \rangle = \delta(f - f') S_h(f)$. The dimensionless characteristic strain amplitude is defined by $h_c^2(f) = f S_h(f)$. Averaging over polarizations of the wave and the orientations of the source relative to the detector, the characteristic strain amplitude from a merger at redshift z is Flanagan & Hughes (1998a)

$$\begin{aligned} h_c(f) &= \sqrt{\frac{2G}{c^3} \frac{(1+z)}{\pi d_L(z)}} \sqrt{\frac{dE}{df_s}} \\ &= 3.56 \times 10^{-26} \left(\frac{\text{Mpc}}{d_L(z)} \right) \left(\frac{1+z}{1+10} \right) \sqrt{\frac{dE/df_s}{M_\odot \text{m}^2 \text{s}^{-1}}}, \end{aligned} \quad (5)$$

where $d_L(z)$ is the luminosity distance to the merging BH pair, dE/df_s is the energy spectrum of the radiation at the source, and $f_s = f(1+z)$ is the frequency at the source. There are four phases of gravity wave emission during the coalescence of a BH pair and we now discuss the energy spectra, dE/df_s , of gravity waves emitted during each phase in turn. We refer to the masses of the two BHs as M_1 and M_2 , with $M_1 > M_2$. Following Flanagan & Hughes (1998a), we refer to the four phases of BH coalescence as *inspiral*, *merger*, *ringdown*, and *decay*. We show these phases schematically in Figure 5 for a single merger of BHs of mass $M_1 = 1.5 \times 10^5 M_\odot$ and $M_2 = 1.1 \times 10^5 M_\odot$ at $z = 13$. These values are typical of the individual mergers in our calculations (see § 3). The thick line in Fig. 5 represents the 5σ detection threshold for a 1 year mission with LISA based on the sensitivity characteristics proposed for the LISA interferometer. We generated this curve and all subsequent sensitivity curves with the LISA *online sensitivity curve generator*⁷. Signals just above threshold and with a well-understood waveform can be culled from the data stream using optimal filtering techniques (e.g. Flanagan & Hughes 1998a); however, it is already clear from Fig. 5 that if our model is correct, LISA should be able to study the predicted gravitational wave background at high signal-to-noise.

First, during the *inspiral* phase, the two BHs are well-separated and lose energy by the self-interaction of the pair with the emitted waves. This radiation-reaction drag causes the two BHs to inspiral slowly toward each other. At this stage, the adiabatic, weak-field limit can be applied in a straightforward way, yielding

$$\begin{aligned} \left(\frac{dE}{df_s} \right)_{\text{Inspiral}} &= \frac{1}{3} \left(\frac{\pi^2 G^2}{f_s} \right)^{1/3} \frac{M_1 M_2}{(M_1 + M_2)^{1/3}} \\ &= 1.86 \times 10^{13} M_\odot \text{m}^2 \text{s}^{-1} \left(\frac{f_s}{\text{s}^{-1}} \right)^{-1/3} \\ &\quad \times \left[\frac{M_1 M_2}{(M_1 + M_2)^{1/3}} \right], \end{aligned} \quad (6)$$

where the BH masses are expressed in M_\odot . The inspiral phase begins at a frequency (equivalently, a physical separation between

⁷ This is available at URL <http://www.srl.caltech.edu/~shane/sensitivity/>

BHs) where the emission of gravitational waves becomes the dominant mode of energy loss and ends at a frequency corresponding to the transition from radiation-reaction-driven inspiral of the two BHs to a free-falling plunge toward each other.

We label the frequency at which inspiral is initiated as f_{\min} , and the frequency at which it ends as f_{merger} . The value of f_{merger} is roughly set at $f_{\text{merger}} \sim 4.1 \times 10^{-3} M_{\text{total},6}^{-1} \text{s}^{-1}$ where $M_{\text{total},6}$ is the total mass in the pair expressed in units of $10^6 M_{\odot}$. Even though the value of f_{merger} may vary up to several percent if the masses involved in the pair are unequal and/or if the BHs are rotating, we choose this conservative value in order to circumvent the need to generate numerical templates that would be required if the frequency were higher (see Flanagan & Hughes 1998a). A low value of f_{merger} is conservative because it *minimizes* the energy emitted per frequency interval during the merger phase (see below), thus minimizing the strain induced during the merger. The value of f_{\min} is rather uncertain. Previous studies assumed it to be a constant (Wyithe & Loeb 2003), or set it to the frequency at the so-called ‘‘hardening’’ radius of the system (Sesana et al. 2004a). We choose to leave it a free parameter, and parameterize it in terms of the variable β , defined as $\beta \equiv f_{\min}/f_{\text{merger}}$. We then examine the sensitivity of our results to the β parameter. We assume that β may take a range of reasonable values between $10^{-3} - 10^{-1}$. These values span the range that the masses of the BHs and host halo properties involved in our calculation imply, had we followed the same procedure as Sesana et al. (2004a).

The time evolution of the emitted frequency of gravitational waves during inspiral is set by the evolution of the orbital frequency of the binary and is given by

$$t_{\text{inspiral}}(f_1 \rightarrow f_2) \simeq 3.2 \times 10^{-3} \text{yr} \frac{(M_1 + M_2)^{1/3}}{M_1 M_2} \left(f_1^{-8/3} - f_2^{-8/3} \right) \quad (7)$$

It is easy to predict the effect of changing β on our results. Choosing f_{\min} very close to the value of f_{merger} ensures that nearly all potential pairs complete the inspiral phase (unless of course they were accreted at very low redshift, see the discussion on t_{mig} in § 3.3). In this case, the central BHs grow by the large number of merger events they experience. On the other hand, if we choose β very small (e.g. $f_{\min} \ll f_{\text{merger}}$), then the time spent in the inspiral phase may, in some cases, approach the Hubble time and most pairs will not merge by $z = 0$. In this case, the central BH does not grow significantly by mergers with incoming BHs.

After the inspiral phase, a BH pair reaches the maximum frequency f_{merger} . The system transitions from an inspiral to a plunge toward each other. This stage of evolution of a binary system is poorly-understood and, following Flanagan & Hughes (1998a), we refer to this as the *merger* phase. The merger is highly non-linear and numerical simulations of this process are not yet accessible. The merger phase is generally rapid (of order minutes, $t_{\text{merg}} \sim 1.47 \times 10^2 \text{s} M_{6,\text{total}}$), and the system quickly evolves to the quasi-normal-ringing phase (see the extensive discussion in Flanagan & Hughes 1998a). The merger event occurs in the frequency interval between f_{merger} and f_{qnr} , where f_{qnr} is the quasi-normal-ringing frequency set by the spin of the resulting BH. The resulting BH may be rapidly rotating even if the individual BHs had very small or zero angular momentum (however, see Hughes & Blandford 2003). We assume a value for f_{qnr} given by the analytic fit of Echeverria (1989) $f_{\text{qnr}} \approx c^3 [1 - 0.63(1-a)^{3/10}] / 2\pi G(M_1 + M_2)$, where a is the dimensionless spin parameter of the resulting BH of mass $M_1 + M_2$. We assume that the spin parameter takes a value of $a = 0.95$, in order to minimize the resulting strain induced from the decay phase of gravitational wave emission (see below). The resulting value of f_{qnr} is then $f_{\text{qnr}} = 2.41 \times 10^{-2} M_{\text{total},6}^{-1} \text{s}^{-1}$. We use an approximation for the energy spectrum from the merger phase presented by Flanagan & Hughes (1998a):

$$\begin{aligned} \left(\frac{dE}{df_s} \right)_{\text{Merger}} &= \frac{\epsilon_{\text{merger}}(M_1 + M_2) \xi(\mu, M_1, M_2) c^2}{f_{\text{qnr}} - f_{\text{merger}}} \Theta_1 \Theta_2 \\ &= 2.7 \times 10^{15} M_{\odot} \text{m}^2 \text{s}^{-1} \left(\frac{\epsilon_{\text{merger}}}{0.03} \right) \\ &\times \frac{(M_1 + M_2) \xi(\mu, M_1, M_2)}{f_{\text{qnr}} - f_{\text{merger}}} \Theta_1 \Theta_2 \end{aligned} \quad (8)$$

where $\Theta_1 = \Theta(f - f_{\text{merger}})$ and $\Theta_2 = \Theta(f_{\text{qnr}} - f)$ are step functions and the masses are in units of M_{\odot} . The function $\xi(\mu, M_1, M_2)$ is the reduction function which ensures correct fitting to numerical calculations for equal and non-equal mass BH pairs. It has the value $\xi(\mu, M_1, M_2) = [4\mu/(M_1 + M_2)]^2$, where μ is the reduced mass of the pair. The quantity ϵ_{merger} is the fraction of the total mass $M_1 + M_2$, released via gravitational radiation during the merger phase. The efficiency at which energy is radiated depends on the mass of the BHs in the merging phase, their individual spins, and their orbital configuration just prior to the merger (generally taken to be the orbital parameters at f_{merger}). Flanagan & Hughes (1998a) estimate ϵ_{merger} based on angular momentum conservation. By assuming an idealized scenario where BH spins and orbital angular momenta are aligned, and assuming that only the quadrupole radiation carries away energy, they estimate a value of $\epsilon_{\text{merger}} \sim 0.1$. However, based on the approach of Smarr (1979), Detweiler (1979) showed that the efficiency can be as low as $\epsilon_{\text{merger}} \gtrsim 0.03$ for merging BHs with no spin. To be conservative, we choose $\epsilon_{\text{merger}} = 0.03$ for the rest of our calculation.

The *ringdown* phase corresponds to damped oscillations of the quasi-normal modes of the resultant BH at the quasi-normal-ringing frequency f_{qnr} . *Decay* is the subsequent emission of decaying gravitational waves as the merged remnant settles toward a Kerr BH (Echeverria 1989). The remnant settles toward a BH with mass that may approach the sum of the two masses $M \lesssim M_1 + M_2$. The actual resulting mass depends upon on the details of the merger which, to date, are poorly understood. An estimate of the energy

spectrum of gravitational waves during the ringdown and decay phases is (Flanagan & Hughes 1998a),

$$\begin{aligned} \left(\frac{dE}{df_s}\right)_{\text{Ringdown}} &= \frac{8c^2}{32\pi^3} \frac{\epsilon_{\text{ringdown}}}{Q f_{\text{qnr}}} \left(\frac{f_s}{\tau}\right)^2 \\ &\times (M_1 + M_2) \xi(\mu, M_1, M_2) B(f_s, f_{\text{qnr}}) \\ &\simeq 9.1 \times 10^{11} M_{\odot} \text{m}^2 \text{s}^{-1} \left(\frac{\epsilon_{\text{ringdown}}}{0.01}\right) \\ &\times (M_1 + M_2) \xi(\mu, M_1, M_2) \\ &\times \left(\frac{16}{Q}\right) \left(\frac{f_s/\text{s}^{-1}}{\tau/\text{s}}\right)^2 \frac{1}{f_{\text{qnr}}} B(f_s, f_{\text{qnr}}) \end{aligned} \quad (9)$$

where masses are expressed in M_{\odot} , Q is the quality factor, and τ the damping time of the quasi-normal ringing mode (assumed to be the $l = m = 2$ mode), and they are related by $Q = \pi f_{\text{qnr}} \tau \approx 2(1-a)^{-9/20}$ (Echeverria 1989). The function $B(f_s, f_{\text{qnr}})$ is defined as

$$\begin{aligned} B(f_s, f_{\text{qnr}}) &= \frac{1}{[(f_s - f_{\text{qnr}})^2 + (2\pi\tau)^{-2}]^2} \\ &+ \frac{1}{[(f_s + f_{\text{qnr}})^2 + (2\pi\tau)^{-2}]^2} \end{aligned} \quad (11)$$

The amplitude of gravitational waves produced at ringdown depends weakly on the value of a . However, the rate at which the induced strain falls off during the decay phase depends on a through the damping time τ . Specifically, the strain amplitude at $f > f_{\text{qnr}}$ is higher for smaller values of τ . The spin parameter generally depends on all of the details of BH formation and merger. To be conservative and minimize the induced strain during merger, ringdown, and decay, we take a constant $a = 0.95$. The quantity $\epsilon_{\text{ringdown}}$ is the fraction of energy released in gravitational waves during ringdown and decay. The amplitude of the gravitational radiation during ringdown, and hence $\epsilon_{\text{ringdown}}$, are not well known. Numerical simulations give $\epsilon_{\text{ringdown}} \sim 0.03$ (Brandt & Seidel 1995). This value can also be obtained under simplifying assumptions about the origin of the waves during ringdown (Flanagan & Hughes 1998a). For lack of any other estimates, and to remain conservative in our approach, we choose a constant $\epsilon_{\text{ringdown}} = 0.01$ ⁸.

4.2. Black Hole Recoils from Asymmetric Gravity Wave Emission and Many Body Interactions

Using the methods described in § 3.1 to § 4.1, we have a complete description of the formation of BH seeds at high redshift, their evolution, and their merger histories notwithstanding a few physical parameters that contain our ignorance of various details. There are two additional effects that serve to complicate the situation and it is necessary to examine the robustness of our results to these effects.

One effect that has been neglected in all but one of the previous analyses (Sesana et al. 2004a) is that BH mergers result in a considerable recoil of the center of mass of the system due to the asymmetric emission of gravitational waves during the final stages of coalescence (Fitchett 1983). Favata et al. (2004) recently addressed this problem in detail and found that expected recoils could be

$$V_{\text{recoil}} \sim [40 - 500] g(M_1/M_2) / g_{\text{max}} \text{ km s}^{-1}, \quad (12)$$

where the dependence upon mass ratio is encapsulated in $g(x) = x^2(1-x)/(1+x)^5$ which reaches of maximum of $g_{\text{max}} \simeq 0.018$ at $x_{\text{max}} \simeq 0.382$. The uncertainty in the normalization reflects the uncertainty in the calculation of the recoil during the final ‘‘plunging’’ stage of BH coalescence and the range we quote corresponds to the *upper limit* and *lower limit* estimates of Favata et al. (2004). The function $g(x)/g_{\text{max}}$ is broad about its maximum, such that $g(x)/g_{\text{max}} \gtrsim 0.1$ for $0.03 \lesssim x \lesssim 0.98$.

The size of the recoil and the mass ratios for which this recoil is sizable are in a range such that they may have a significant effect on our results. Figure 3 shows that the majority of BH mergers commence around $z \sim 10$. In this first series of mergers there are no supermassive BHs and mass ratios typically are from $0.06 \lesssim M_2/M_1 \lesssim 0.9$ (e.g. Figure 4). The first series of mergers occurs in systems that are roughly $M_{\text{vir}} \sim 100 M_{\text{v,crit}} \sim 10^{10} h^{-1} M_{\odot}$. For halos described by the NFW density profile, the escape velocity from the halo center V_{esc} , is related to the maximum circular velocity attained by the density profile V_{max} , by $V_{\text{esc}} \simeq 3V_{\text{max}}$. Typical values for this mass and redshift range are $V_{\text{max}} \sim 75 \text{ km s}^{-1}$ so that $V_{\text{esc}} \sim 225 \text{ km s}^{-1}$. Thus, in most halos of interest, the velocity kick can likely be a significant fraction of the halo escape velocity or more, implying that the BH remnants are ejected from the halo centers.

We estimate the potential impact of the gravitational radiation recoils on our results in the following way. For each merging pair, we assign the remnant a recoil speed set by the *upper limit* in Equation (12). For nearly $\sim 70\%$ of our BH mergers, recoils of this magnitude allow the remnant to escape from the halo. We cease to track escaped remnants. Even for the remainder, the velocities are typically large enough that the ejected remnants make excursions that are a large fraction of the scale radius of the host halo profile ($\gtrsim 0.3r_s$). In this case it may be possible for some mechanism to return the remnants to the centers of halos rapidly, where they may experience further mergers; however, our simple model contains no such mechanism. In effect, the recoils cause our seed BHs to merge once with further merger activity effectively shut off. Therefore, this approach results in a minimum expected gravity wave signal from seed BHs formed according to the KBD mechanism by allowing each black hole to merger once at most.

We note that for recoils of this size and in the absence of an efficient mechanism to return merger remnants to their halo centers, SBHs cannot be built up efficiently through mergers. Instead, this case of a strong gravity wave recoil results in a population of ‘‘orphaned’’ BHs wandering in the intergalactic medium, similar to the study of Volonteri et al. (2003).

⁸ During the preparation of this manuscript, Sperhake et al. (2005) reported the results of a new calculation based on mesh-refinement and dynamic singularity excision where they estimated the fraction of the total ADM mass of a merged system that is radiated during ringdown to be $\sim 0.1\%$.

In our fiducial models, we neglect the effect of three-body interactions on merging black holes. This occurs when a third BH falls into the coalescing BH binary at the halo center prior to completion of the BH merger. The general effect of such interactions is that the lowest-mass BH of the three is ejected from the system with the consequence that the remaining binary is left more tightly bound than before (Hills & Fullerton 1980). We estimate the importance of potential three-body interactions in the following way. We trace through our merger trees and determine the fraction of events for which a third BH falls within the inspiral radius of an existing binary before the existing binary has had time to merge according to t_{inspiral} in Eq. (7).

For our fiducial model, we find that this occurs in only $\sim 0.4\%$ of BH mergers, so neglecting this effect is a reasonable approximation. We note that our estimates are in broad agreement with those of Islam et al. (2004c), which is not surprising because our model of halo evolution is similar to the model that they employ. However, Volonteri et al. (2003) found three-body interactions to be non-negligible in their analysis. The discrepancy is likely due to the fact that Volonteri et al. (2003) do not account for tidal mass loss from subhalos, thus greatly decreasing the dynamical friction infall timescale of a subhalo. In addition, a secondary effect is the fact that higher order subhalos in the merging tree may be stripped from infalling subhalos due to the tidal field of the main host system (see Zentner et al. 2005, for a complete discussion), an effect not taken into account in Volonteri et al. (2003). Even in the presence of three-body interactions, we expect that our model which includes maximal velocity recoils, should represent a lower bound on the predicted gravity wave background, because it allows each black hole to merge, at most, once.

4.3. The Gravity Wave Background from Black Hole Mergers

We calculate the energy spectra for each merger as described previously in Section 4.1. For each potential pair, we calculate f_{merger} at the source (which depends only on the BH masses). Then, using our adopted values of t_{mig} and β , we compute the well-understood time evolution of the emission frequency during inspiral using Eq. (7) and determine the observed values of f_{min} and f_{merger} . We then estimate the duration of the merger and the observed value of f_{qnr} . The relations in the previous subsection then yield the energy spectrum for each merger event. We present results for the total spectrum as well as the signals from inspiral, merger, and ringdown and decay which we treat together. We now describe how we compute the gravity wave background from these spectra.

We compute the total gravity wave background using our Monte Carlo merger tree realizations. Averaging over the merger tree realizations at a fixed final host mass allows us to compute the mean energy spectrum due to all BH pairs emitting gravitational radiation in a redshift range dz about z , associated with progenitors of a halo of mass M_{vir} today. We denote this quantity $d\bar{E}_{\text{gw}}(z, M_{\text{vir}})/dzd\ln f_s$, where $f_s = f(1+z)$ is the frequency at the source. The levels of stochastic gravity wave backgrounds are often quoted in terms of the energy density in gravity waves per logarithmic frequency interval measured in units of the critical energy density of the universe, $\Omega_{\text{gw}}(f)$. We compute the comoving energy density in gravity waves by integrating $d\bar{E}_{\text{gw}}/dzd\ln f_s$ over redshift and halo mass,

$$\begin{aligned} \rho_c c^2 \Omega_{\text{gw}}(f) &= \int \int \frac{dn(M_{\text{vir}}, z=0)}{d\ln M_{\text{vir}}} \\ &\times \frac{d\bar{E}_{\text{gw}}(z, M_{\text{vir}})}{dzd\ln f_s} (1+z)^{-1} dz d\ln M_{\text{vir}} \end{aligned} \quad (13)$$

In Equation (13), $dn(M_{\text{vir}}, z=0)/d\ln(M_{\text{vir}})$ is the comoving number density of halos per logarithmic mass interval evaluated at redshift $z=0$. We assume that this function takes the form proposed by Sheth & Tormen (1999). Formally, the integral over $\ln M_{\text{vir}}$ should be taken from $\ln M_{\text{vir}} = [-\infty, \infty]$. In practice, we compute the integrand at discrete values of M_{vir} as described in Section 3.2. We then compute the integral using a power-law interpolation of $d\bar{E}_{\text{gw}}(z, M_{\text{vir}})/dzd\ln f_s$ to evaluate the integrand of Eq. (13) between neighboring bins of M_{vir} . Once the energy density of the gravitational wave background is known, we can relate this back to the characteristic strain by

$$h_c^2(f) = \frac{4G\rho_c}{\pi f^2} \Omega_{\text{gw}}(f), \quad (14)$$

so that

$$h_c(f) \simeq 8.8 \times 10^{-19} \Omega_{\text{gw}}^{1/2}(f) \left(\frac{\text{s}^{-1}}{f} \right). \quad (15)$$

In the Section 5, we present our results for the gravity wave background due to mergers between seed BHs in terms of the $h_c(f)$.

4.4. Is The Gravity Wave Background Resolvable or Stochastic?

The background of gravity waves that we compute in Section 4.3 is a sum of contributions from numerous individual mergers. It is important to determine whether the background of gravity waves that any merger scenario predicts can be resolved into discrete events. In this section, we outline our method for determining whether our predicted signals are stochastic in nature, or resolvable.

Generally speaking, the gravity wave signal from a particular event can be considered “resolved” if it is detected above some rms signal-to-noise ratio, $\langle S/N \rangle$. This signal-to-noise ratio describes the likelihood of misinterpreting fluctuations in the instrumental noise or any known backgrounds that might be included in the calculation as the signal from the gravity wave source. In the case of a gravitational wave detector, the instrumental noise is quantified by the noise spectrum of the particular instrument (e.g., see Thorne 1987, 1996; Larson et al. 2001). Given a population of sources, we can estimate whether these sources will be resolved or not, by counting the number of sources that are above a certain $\langle S/N \rangle$ in a given frequency bin Δf . The frequency resolution is set by the length of the observation time τ_{obs} , as $\Delta f = \tau_{\text{obs}}^{-1}$.

Recently, Cornish (2003) showed that a realistic criterion for a background signal, built from a sum of a number of individual events or sources, to be stochastic and unresolvable into individual sources is when there is more than one gravity wave source above

a particular $\langle S/N \rangle$ per \sim eight frequency resolution bins, the so-called *eight-bin rule*. In what follows we use the eight-bin rule to determine whether our models predict resolvable or stochastic gravity wave backgrounds.

For a gravity wave source inducing a characteristic strain $h_c(f)$, the signal-to-noise ratio at a frequency f , averaged over the orientation of the detector is given by (see Flanagan & Hughes 1998a, for a derivation),

$$\begin{aligned} \langle S/N \rangle_{\Delta f} &= \sqrt{\int_f^{f+\Delta f} \frac{h_c^2(f)}{h_{\text{noise}}^2(f)} \frac{df}{f}} \\ &= 3.24 \times 10^{-27} \frac{(1+z)}{d_L(z)} \sqrt{\int_f^{f+\Delta f} \frac{dE/df_s}{h_{\text{noise}}^2(f)} \frac{df}{f}}. \end{aligned} \quad (16)$$

In Equation (16), the luminosity distance to the source is in units of Mpc, and dE/df_s , the energy spectrum at the source, is in units of $M_\odot \text{m}^2 \text{s}^{-1}$. The quantity $h_{\text{noise}}(f)$ is the rms noise of the detector for sources at random directions and orientations. We assume a LISA sensitivity curve appropriate for an exposure time of 3 years. In this case, the frequency resolution bin has a width of $\Delta f \approx 10^{-8} \text{s}^{-1}$.

We estimate the number of sources per eight frequency resolution bins in the following way. We first calculate the mean number of events per redshift interval from z to $z+dz$, contributing above a specified $\langle S/N \rangle$, in a frequency bin, for each bin halo mass in our merger tree realizations. We denote this quantity as $d\bar{N}(M_{\text{vir}}, z)/dz$. We then calculate the mean number of events per comoving volume and time as

$$\frac{d\bar{N}}{dV dt} = \int_0^\infty \frac{d\bar{N}(M_{\text{vir}}, z)}{dz} \left| \frac{dz}{dt} \right| \frac{dn(M_{\text{vir}}, z=0)}{dM_{\text{vir}} dV} dM_{\text{vir}}. \quad (17)$$

Here, dz/dt is given by $dz/dt = -(1+z)H_0\sqrt{E(z)}$, where $E(z) = (1+z)^2(1+\Omega_M z) - z(2+z)\Omega_\Lambda$ and H_0 is the present value of the Hubble constant. We evaluate the integral using the same power-law interpolation scheme that we used to evaluate the integral in Eq. 13 above. From this quantity, we then estimate the total number of events observed per observed time as

$$\frac{d\bar{N}}{dt_{\text{obs}}} = \int_0^\infty \frac{d\bar{N}}{dV dt} \frac{dV}{dz} \frac{dz}{1+z}. \quad (18)$$

The total number of observed events in an observation time τ is then simply

$$N_{\text{total}} = \int_0^\tau \frac{d\bar{N}}{dt_{\text{obs}}} dt_{\text{obs}}. \quad (19)$$

In Eq. 18 the quantity dV/dz is the comoving volume in a redshift interval between z and $z+dz$ and is given by

$$\frac{dV}{dz} = 4\pi \left(\frac{c}{H_0} \right)^3 \frac{1}{\sqrt{E(z)}} \left(\int_0^z \frac{1}{\sqrt{E(z')}} dz' \right)^2. \quad (20)$$

5. RESULTS

5.1. Stochasticity

Our first result addresses the issue of the stochasticity of the gravity wave background. As described in § 4.4, we calculate the number of individual black hole merger events that are above a given signal-to-noise ratio and assess stochasticity according to the eight bin rule. Figure 6 shows this result for the different variants of the KBD model that we study. Clearly, for a threshold signal-to-noise ratio of $\langle S/N \rangle = 1$, the number of sources per eight frequency bins in our fiducial scenario is quite large in the frequency range $10^{-2} \text{s}^{-1} \gtrsim f \gtrsim 10^{-5} \text{s}^{-1}$. This implies that the individual mergers will generally not be resolvable and that the gravity wave background is stochastic in nature over this frequency range. However, at a threshold signal-to-noise ratio of $\langle S/N \rangle = 5$, the gravity wave background becomes resolvable after 3 years of observation. In this case, the background is stochastic only in the small frequency range $2 \times 10^{-3} \text{s}^{-1} \gtrsim f \gtrsim 7 \times 10^{-4} \text{s}^{-1}$. Therefore, for low detection thresholds, the gravity wave background from a KBD-like model is stochastic, while for high detection thresholds it will be resolvable into individual merger events.

The reason for the large number of sources in this scenario is easily understood. In models with large seeds, most pairs of black holes contribute a substantial gravity wave signal in the frequency range probed by an instrument like LISA. The gravity wave signal in high-mass seed black hole models is dominated by mergers between seeds just after formation, when the merger rate of halos and black holes is high (see Fig. 3 and Fig. 4) and we will return to this point in the following section. Models based on the MR01-type scenario predict that the gravity wave background will be resolvable, even at a relatively low signal-to-noise ratio threshold of $\langle S/N \rangle \sim 1$. The reason is because only a relatively smaller number of black hole pairs in that scenario emit gravity waves in the LISA frequency range with large amplitudes. In models with low-mass seeds, supermassive black holes grow predominantly through accretion, and do not reach masses that contribute significantly to the LISA frequency range until relatively low redshift.

5.2. The Gravitational Radiation Background

In this subsection, we present our estimates of the gravitational wave background produced by the merging of high-mass seed BHs formed at high redshift. Our primary result regarding the gravitational wave background from BH mergers is shown in Figure 7. This Figure shows the full gravity wave spectrum from BH mergers as well as a decomposition of the gravity wave spectrum into contributions from the different phases of BH coalescence and merger. This decomposition may be useful, for example, because the inspiral phase is understood significantly better than the subsequent phases of the merger, where numerical relativity is needed. We

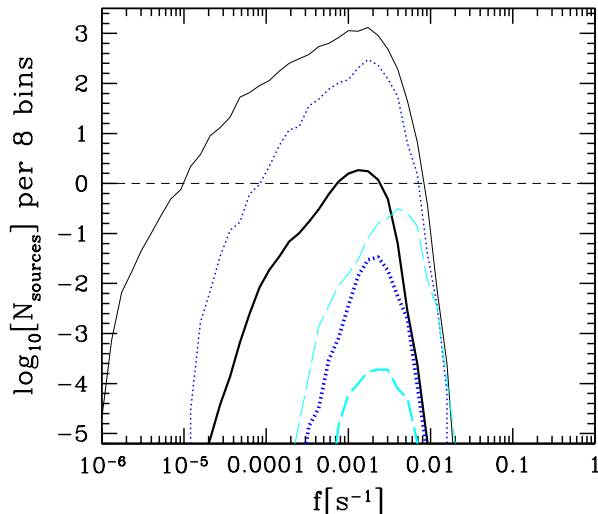


FIG. 6.— The number of black holes per eight frequency resolution bins for a 3 year observation time with LISA. *Thick* lines correspond to the number of sources with $\langle S/N \rangle \geq 5$, while *thin* lines represent the number of sources with $\langle S/N \rangle \geq 1$. *Solid* lines depict the number of sources in the fiducial case where the migration timescale is $t_{\text{mig}} = 10 \text{ Myr}$, $\beta = 10^{-1}$ and reionization occurs at $z_{\text{re}} = 12$. The *dotted* line corresponds to the same set of parameters with the inclusion of the effect of radiation recoil described in § 4.2. The *short, dashed* line corresponds to the extreme scenario where radiation recoil is included, the redshift of reionization is set at $z_{\text{re}} = 16$ and the seed black hole masses are reduced by two orders of magnitude from the fiducial KBD mass (see § 5.2).

also show the variation of our predictions with the two parameters that our model is most sensitive to, the redshift of reionization z_{re} , and the degree importance of radiation recoil after BH mergers. We present the background in terms of the characteristic strain induced as in Eq. 15. In each panel of Fig. 7, we also show the LISA sensitivity to bursts computed using noise spectral densities from the LISA *online sensitivity curve generator*) after a three year exposure (Thorne 1987, 1996; Larson et al. 2001).

It is apparent from the results in Fig. 7, that the background that we predict is considerable compared to the expected LISA instrumental sensitivity and that, if this model is correct, LISA should be able to measure this spectrum at very high signal-to-noise ratios. Limits on pulsar timing residuals constrain the energy density in a stochastic gravitational wave background to roughly $\Omega_{\text{gw}}(f) \lesssim 4 \times 10^{-9}$ in the frequency range $10^{-9} \lesssim (f/\text{s}^{-1}) \lesssim 10^{-8}$ (Lommen 2002). Our models are not constrained by these bounds because the spectra that we predict peak around typical frequencies of $f \sim 10^{-4} - 10^{-2} \text{ s}^{-1}$ and fall off rapidly on either side of the peak.

As we describe in more detail below, varying the unknown parameters in the calculation within reasonable ranges does not change our basic result. We are left with the promising result that LISA should be able to confirm or essentially to rule out classes of models based on the formation of massive seed BHs because a considerable gravity wave background is one of the generic predictions of such a scenario. LISA should be able to observe the relatively simple, well-understood phase of BH binary inspiral over more than 3 orders of magnitude in frequency.

Most previous studies employed significant growth of central BHs through accretion (Sesana et al. 2004a,b). In our model we do not include such a prescription, for two reasons. First, we would like to examine the robustness of the KBD model and its predicted gravitational wave spectrum. The spectrum would only be boosted by additional accretion onto central BHs. Secondly, current prescriptions for accretion onto BHs that grow via mergers are uncertain and must be tuned in order to reproduce observed correlations at $z = 0$ (e.g. Volonteri et al. 2003). Nevertheless, specific prescriptions for accretion can easily be incorporated into the framework of our calculation should growth through accretion become more well understood.

The general shape of the gravity wave spectrum can be understood in the following way. As the frequency of emission depends on the mass of the pair, the high-frequency regime is dominated by the mergers of relatively low-mass BHs with the original seed BH mass, while the low-frequency regime originates from the merger of more massive pairs. The spectrum drops steeply at the high-frequency end for two reasons. First, the spectra from individual mergers drop sharply at a maximal frequency set by the mass scale of the merging black holes, in this case the mass scale of the KBD seed BHs (see § 4.1). Second, due to the hierarchical build-up of SBHs that we describe in this study, small masses contribute primarily at higher redshifts than high-mass BH pairs (see Figure 4). The frequency of emitted radiation by small mass BHs experiences a larger redshift toward lower frequencies than that from corresponding pairs of larger mass BHs, resulting in a steepening of the gravity wave spectrum at high frequencies. The apparent cutoff that is seen at low frequencies basically reflects an upper limit on the resulting mass of BHs at $z = 0$. If the BH masses at $z = 0$ are the result of merging of smaller mass BHs as we assume in this study, then this mass is directly proportional to the mass of seed BHs as well as the number of mergers that occurred in the process of forming the BH at $z = 0$. The sharpness of the cutoff results from our choice of a fixed value of the parameter $\beta = f_{\text{min}}/f_{\text{merger}}$. If instead we were able to assign a different value of β for each one of the coalescing pairs, then the decline at lower frequencies would be smooth. Our choice of a fixed value of β for all pairs simplifies the calculation but does not change the essential results (see below).

We emphasize that our results are robust to variations of the migration timescale t_{mig} . We can understand this directly from Fig. 3

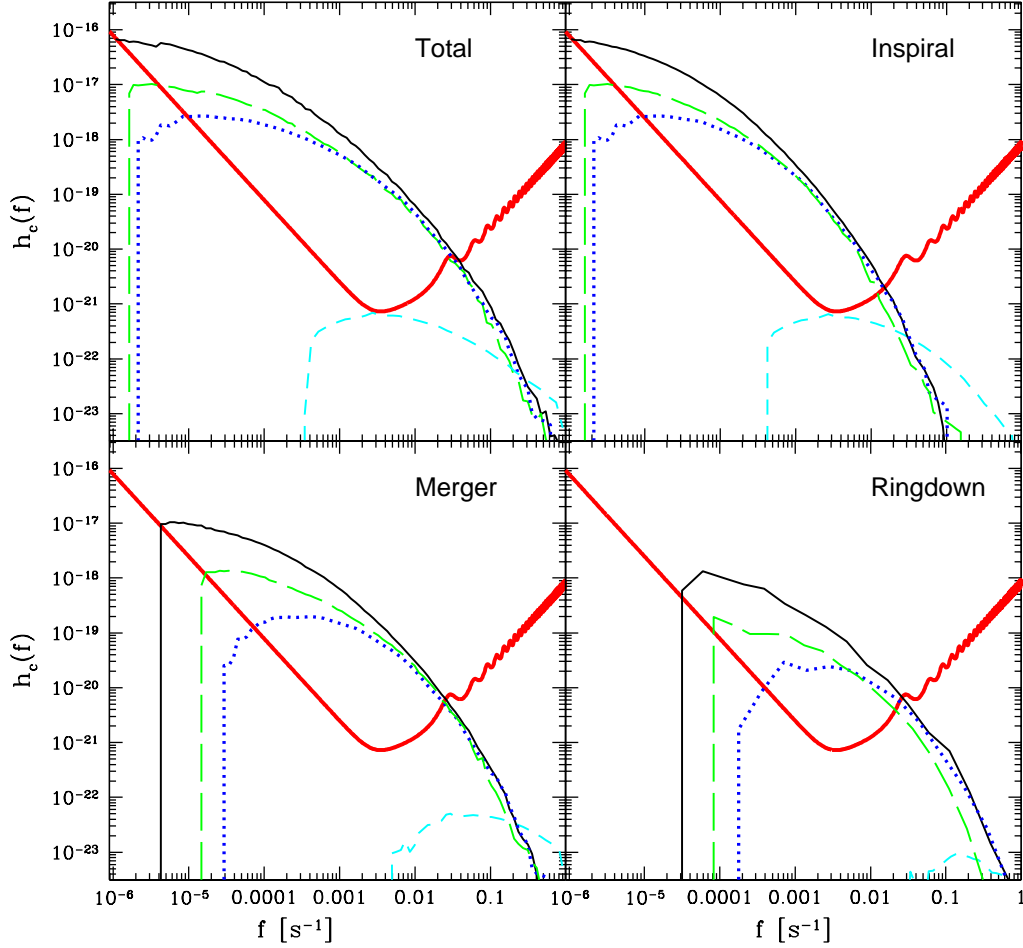


FIG. 7.— The spectrum of the gravity wave background induced by the hierarchical merging of massive BH seeds. The *upper, left* panel shows the total gravity wave background while the other three panels show the background decomposed into contributions from mergers in the *inspiral, ringdown and decay, and merger* phases (proceeding clockwise from the upper left). In each panel, the *thick, solid* line that rises steeply at high frequency represents the LISA sensitivity to gravity wave bursts (Thorne 1987, 1996; Larson et al. 2001) computed using the LISA *online sensitivity curve generator*. The *thin, solid* lines correspond to the gravity wave background in our fiducial model with $z_{\text{re}} = 12$, $t_{\text{mig}} = 10$ Myr, and $\beta = 10^{-1}$. The *dotted* lines correspond to the same set of parameters with the inclusion of the effect of radiation recoil described in § 4.2. The *long-dashed* line corresponds to the same choice of parameters except for the redshift of reionization, which is set to $z_{\text{re}} = 16$, and with no radiation recoil. The short-dashed line corresponds to an extreme scenario with maximum radiation recoil included, a redshift of reionization set at $z_{\text{re}} = 16$, and the seed BH masses reduced *artificially* by two orders of magnitude from the fiducial KBD mass scale.

and Fig. 4. These Figures show that most of the potential BH pairs in this model are formed quite early on ($z \gtrsim 10$) and, moreover, that many of these mergers are between the near-equal-mass seed BHs. Thus, most pairs have of order \sim many Gyr to evolve toward inspiral and begin emitting appreciable gravity waves. Varying t_{mig} from 1 Myr to 1 Gyr results in only a small reduction in the gravitational wave background. Only pairs that merge at redshifts $z \lesssim 0.1$ are excluded by this criterion and the number of these pairs is comparably quite small, as can be gleaned from Fig. 3. The only way to reduce significantly the signal would be to require migration times in excess of a Hubble time.

Similarly, lowering the minimum frequency (or equivalently, increasing the maximum binary separation) at which gravitational radiation becomes the primary channel for energy loss, parameterized by $\beta \equiv f_{\text{min}}/f_{\text{merger}}$, allows BH binaries to spend more time evolving through the inspiral phase, boosting the low-frequency signal, which is dominated by inspiral, and reducing the high-frequency signal, where the subsequent phases of merger, ringdown, and decay dominate. Varying the value of β from 10^{-1} to 10^{-3} results in, at maximum, an increase of $h_c(f)$ by a factor of ~ 3 in the low-frequency regime. On the other hand, increasing the value of β up to 5×10^{-1} , the decrease in the characteristic strain is at most a factor of 2. Therefore, varying the values of t_{mig} and β within their expected ranges does not significantly alter the main result of this study.

As we have already mentioned, unlike the parameters β and t_{mig} , the gravity wave spectrum is sensitive to the redshift of reionization, z_{re} (or any other cosmological epoch that effectively terminates the KBD process). In our fiducial model, we follow KBD and adopt a value of $z_{\text{re}} = 12$, which is shown by the thin, solid lines Fig. 7. Taking a higher reionization redshift, as indicated by the cosmic microwave background polarization anisotropy (Spergel et al. 2003; Page et al. 2003), significantly reduces the low-frequency signal. The dashed lines in Fig. 7 show the results for the KBD model with $z_{\text{re}} = 16$. In the frequency range of interest, the strain spectrum in this case is decreased by at most an order of magnitude relative to the fiducial case. Notice that in the frequency range at which LISA is most sensitive ($10^{-3} \lesssim (f/\text{s}^{-1}) \lesssim 10^{-2}$), the relative decrease is much smaller. The dominant reason for the reduction in the background at low frequency is that there are considerably fewer seed BHs in a model where the KBD mechanism is cut off at this high a redshift (see § 3.1).

Most previous studies have assumed that central BHs merge, one after the other, with infalling BHs. Favata et al. (2004) point out that this may not necessarily hold because the gravity waves emitted during the merger are not emitted isotropically and may induce a recoil on the center of mass of the system that can be large compared to the escape velocities from typical dark matter halos. In this case, BHs can continue to merge *only* if some mechanism returns them to the centers of halos. We estimated the affect of this recoil on our predicted spectrum by allowing BHs to recoil with the *maximum* recoil velocity estimated in Favata et al. (2004). In this scenario, seed BHs effectively merge once and are then cut off from further mergers.

At the low frequency end (see Fig. 7), the spectrum in the recoil scenario is roughly an order of magnitude lower than in our fiducial model; however, the reduction is significantly less at higher frequencies, particularly at the trough in the LISA noise spectrum. The signal should still be detectable at high signal-to-noise by LISA at frequencies in excess of a few $\times 10^{-5} \text{ s}^{-1}$. Again, the reason that this model is robust to the recoils is simple. In this seed BH formation scenario, BHs start with very large masses ($\sim 10^5 M_{\odot}$) compared to the MR01-motivated models ($M_{\text{BH}} \sim 10^2 M_{\odot}$). Mergers between these seeds already produce a sizable strain compared to the LISA noise curve. Therefore, even if the aggregation of BHs is cut-off after a single merger due to the recoil, the gravity wave background may still be quite large in the frequency regime that LISA will probe most reliably.

Finally, we present results for an extreme scenario that represents the minimal signal that can result from the type of BH formation model that we study here. In this extreme case, we include the maximum velocity recoil and the redshift of reionization is set to $z_{\text{re}} = 16$. In addition, we assume that the initial mass spectrum of BHs (see Fig.2) is shifted to smaller mass by a factor of 10^{-2} . In this case, the characteristic BH mass is of order $M_{\text{BH}} \sim 10^3 M_{\odot}$. In our estimate, we make this shift artificially, simply by resetting the KBD masses, but physically such a shift may be due to some unknown efficiency parameter associated with the formation of very massive BHs. In the case of the KBD model, seeds of this low mass would primarily form if only $\sim 1\%$ of the mass that loses its angular momentum within ~ 10 Myr actually collapses into a black hole. The resultant gravity wave signal from this extreme model is represented by the short-dashed lines in Fig. 7. The gravity wave background is significantly smaller in this model. Notice that because the BHs are smaller and there is minimal growth of BH mass via mergers, the low-frequency signal is essentially gone. However, if supermassive black holes are formed from such an extreme case of the KBD model, the dominant mode of SBH growth must be through accretion.

In general, we note that the backgrounds presented here may still compete with other hypothetical backgrounds associated with, for example, galactic and extragalactic white dwarf binaries (Nelemans et al. 2001; Farmer & Phinney 2003), the formation of the first generation of stars (Schneider et al. 2000), supernovae (Buonanno et al. 2005) or excitations of additional degrees of freedom in theories of spacetimes with large extra dimensions (Hogan 2000),

5.3. Number of resolvable events

As we showed in section § 4.4, the gravity wave background will be resolved into individual sources with a signal-to-noise ratio of greater than 5 for most of the LISA frequency range. We can therefore estimate the number of sources that will be resolved in a given observation time. We assume as before that this time is 3 years, and we estimate the number of sources that are resolved in each one of the phases of gravity wave emission for each pair. We do this in the following way. For each potential pair, we estimate the signal-to-noise ratio for the inspiral and merger phases using Eq. (16). For the inspiral phase, we define the frequency interval Δf , as the difference between f_{merger} and the frequency that the binary was emitting, 3 years (the observation time) before reaching f_{merger} (estimated using Eq. (7)). We perform the integral over frequency in Eq. (16) and determine whether the signal-to-noise ratio meets the requirement $\langle S/N \rangle \geq 5$. For the merger phase, we perform the integral in Eq. (16) with $\Delta f = f_{\text{qnr}} - f_{\text{merger}}$. In the case of the ringdown phase, we approximate the energy spectrum as a δ -function at the ringdown frequency, following the analysis of

Flanagan & Hughes (1998a). In this case the signal-to-noise ratio is given by

$$\begin{aligned} \langle S/N \rangle_{\text{ringdown}} &= 3 \times 10^{-13} (1 + z_{\text{qnr}}) \\ &\times \frac{\sqrt{\epsilon_{\text{ringdown}} f_{\text{qnr}} \xi(\mu, M_1, M_2) M_{\text{total},6}^3}}{f(a) d_L(z) h_{\text{noise}}[f_{\text{qnr}}/(1 + z_{\text{qnr}})]} \end{aligned} \quad (21)$$

where $f(a) = 1 - 0.63(1 - a)^{3/10}$, and a is as usual the dimensionless spin parameter. We perform these $\langle S/N \rangle$ estimates for each pair in all halo masses of our merger tree realizations. We then calculate the mean number of events per redshift interval, $d\bar{N}(M_{\text{vir}}, z)/dz$, and follow the analogous sequence going from Eq. (17) to Eq. (19) to get the total number of events with $\langle S/N \rangle \geq 5$ in a 3 year of observation with LISA.

We find that for our fiducial case with $z_{\text{re}} = 12$, $t_{\text{mig}} = 10 \text{ Myr}$ and $\beta = 10^{-1}$ that in a 3 year integration, LISA should be able to measure ~ 400 inspiral, ~ 2300 merger and ~ 1100 ringdown events above a signal-to-noise ratio of $\langle S/N \rangle \geq 5$. For the case with the same set of parameters but including also the effects of radiation recoil described in section § 4.2, the corresponding number of resolved events in the inspiral, merger and ringdown phases is 250, 700 and 500 respectively, while for the extreme scenario with maximum radiation recoil, a redshift of reionization of $z_{\text{re}} = 16$ and seed BH masses which are two orders of magnitude lower from the fiducial KBD mass scale these numbers are 1, 60 and 0.1. In all cases, the number of merger and ringdown events is higher than the number of inspiral events. The reason is due to the fact that most of the black hole masses involved (see Fig. 3 and Fig. 4) are such that the signal-to-noise ratio during merger and ringdown is generally larger than the signal-to-noise of inspiral. There are two reasons for this. The inspiral signal-to-noise ratio is roughly a factor $\sim M_1 M_2 / (M_1 + M_2)^2$ smaller than the signal-to-noise ratio for merger and/or ringdown events and, in many cases, inspiral binaries do not enter the LISA sensitivity range until only few weeks prior to the merger and subsequent ringdown phase⁹.

As with the gravity wave spectrum, the numbers of resolved events reflect the underlying characteristics of the KBD model. Massive seed black holes which are formed early experience a large number of mergers. In addition, the seed masses are such that the emitted gravity wave radiation is in the frequency range of a space detector such as LISA. In supermassive black hole formation scenarios which are based on the MR01 model for seed BH formation, seed masses are generally small. As such, the emitted radiation does not move into the LISA frequency range until relatively lower redshifts, at which time the merger rate of the halos that host black holes is significantly decreased. Thus, just as the gravity wave background, the number of resolved events in MR01 models is generally significantly smaller than what is found in KBD-type high-mass BH seed models.

6. CONCLUSIONS

In this paper, we studied the theoretical gravitational wave background predicted by models where supermassive black holes form from a population of high mass seeds and models where mergers are an important channel of SBH growth. We studied as a particular example, the supermassive BH seed formation scenario of Koushiappas et al. (2004). Our primary results can be summarized as follows.

1. The KBD seed BH formation scenario makes a *generic and testable* prediction of a very large gravity wave background that should be resolvable at high signal-to-noise by a space gravity wave detector such as the proposed LISA interferometer. This prediction is insensitive to many of the details of the model. In addition, we have neglected any model of BH growth via accretion which would serve to increase the signal. This has the important implication that instruments with LISA characteristics should be able to confirm or to rule out the KBD scenario and similar models with high mass BH seeds and that future gravity wave detectors should be able to help assess the importance of mergers in the formation of SBHs and the establishment of the observed correlations between the black hole mass and the properties of its host spheroid and halo. Moreover, if the background is detected, an instrument like LISA may be able to study the spectrum in detail providing constraints on some of the uncertain aspects of the model.
2. In general, the detectability of the predicted gravitational wave background is not sensitive to the details of the mechanism of BH migration if BH seeds are formed at high redshift. As long as migration occurs on a timescale less than H_0^{-1} , gravity waves from the inspiral phase of the mergers should still be observable.
3. For KBD-like models with an initial mass function of BH seeds that has a typical mass scale of $M_{\text{BH}} \gtrsim 10^3 M_\odot$, the gravity wave signal is robust to shifts in the redshift of reionization and a very generous reduction in the number of mergers due to radiation recoil effects and three body interactions.
4. While the magnitude of the gravity wave background means that it provides a means of testing BH formation mechanisms, such a signal would also represent a significant background contaminant for any future low-frequency, gravity wave observatories such as BBO or DECIGO (Seto et al. 2001). The gravity wave signal due to models of high-mass seeds would represent a potentially large stochastic background because any such instrument would have a greater sensitivity than LISA. This large background may then inhibit such detectors from achieving their aims of detecting the stochastic gravity wave backgrounds produced during inflation (e.g. Turner 1997), from a first generation of supernovae (e.g. Buonanno et al. 2005), or perhaps from other nonstandard physics (e.g. Hogan 2000).

⁹ for detection schemes in this case, see the extensive discussion in Section VI of Flanagan & Hughes (1998a).

5. The modeling that we present here can be used to provide detailed predictions for the gravity wave signals from a wide class of models of BH formation and their subsequent growth (including growth via accretion) and merging.

A detection of a gravitational wave background will be an enormous discovery in and of itself. One important reason is that it will open up a new window with which to observe the high-redshift universe. We showed that such a detection may yield important information about the formation and subsequent evolution of supermassive BHs. The presence of a background similar to our predictions would suggest the presence of numerous merger events, providing indirect evidence for a high merger rate of massive BHs. However, it is hard to disentangle the merger rate from any signal because of a degeneracy between the BH masses and the redshifts that gravitational waves are emitted (Hughes 2002) unless independent redshifts measurements can be made. Though this may be possible for individual merger events, in the case of a stochastic background this remains an outstanding difficulty.

Further information may be gleaned if spectral features are present in the spectrum. In this calculation, we neglected the gravitational wave emission that may result from the initial collapse of the seed BHs. This could result in the presence of a broadened “emission line” at a frequency which would correspond roughly to the redshifted quasi-normal-ringing frequency of the initial BH seed, and constrain the mass of seed BHs (see Fryer et al. (2002) for a discussion of the gravitational wave emission from collapsing objects). If the background could be measured at high signal-to-noise, the broadening of the line would provide information on the redshift of seed BH formation as well as the spectrum of seed BH mass, while the amplitude of the feature would indicate the abundance of the host halos that harbor the seed BHs (Koushiappas & Zentner 2005).

A non-detection of this predicted background would place very strong limits on the viability of the model proposed by Koushiappas et al. (2004) and similar models of SBH formation from high-mass seeds. Most notably it would severely constrain the mass and abundance of seed BHs. If this background were not detected, then BH seeds would be required to be significantly smaller than the seeds proposed by KBD ($M_{\text{BH}} \lesssim 10^3 M_{\odot}$) or significantly scarcer. Lack of a detection would indicate that growth via mergers of numerous pairs is not the dominant growth mechanism of SBHs and that KBD seed BHs must be so rare that they play, at most, a very limited role in the formation of SBHs in the centers of galaxies. In this case, growth via accretion would have to be the dominant growth mechanism. If, in fact, this is the case, then there might be consequences for the spin evolution of BHs as was pointed out by Volonteri et al. (2005).

These points demonstrate how a gravity wave detector like LISA will open a fundamentally new window on the high-redshift universe, providing a wealth of information on the formation and growth of supermassive black holes and probing the physics of galaxy formation. LISA will probe galaxy formation processes at very high redshift, a task not attainable by other forms of observation except for possibly 21 cm emission (e.g. Zaldarriaga et al. 2004). Supermassive BHs and their formation are directly linked to the formation of galaxies. Information gained from the gravitational wave background induced from BH mergers will inevitably provide useful constraints on high-redshift galaxy formation and insight into the processes that set the observed correlations between supermassive BHs and their hosts. An instrument with the sensitivity and frequency range similar to LISA will be able to confirm, disprove, or distinguish between mechanisms of SBH formation that produce otherwise identical predictions at $z = 0$ (a not uncommon situation as many models have tunable parameters). We demonstrated in this manuscript how LISA will be able to distinguish between the gravitational wave background induced by the KBD model seed BHs and the models that stem from the MR01 scenario. However, the new observational window on the universe that space-based gravity wave detectors will provide promises many further constraints on the fundamental processes of galaxy formation at high redshift.

We thank the anonymous referee for numerous useful suggestions that improved the quality of this manuscript. We are pleased to thank John Beacom, James Bullock, Neal Dalal, Daniel Holz, Scott Hughes, Stelios Kazantzidis, Andrey Kravtsov, Pantelis Papadopoulos, Eduardo Rozo, Gary Steigman, Louis Strigari, Frank van den Bosch, Terry Walker, Casey Watson, David Weinberg and Simone Weinmann for many helpful comments. We would like to thank Gianfranco Bertone for many useful conversations throughout the course of this work and Mark Knopfler for constant support. We acknowledge use of the *online sensitivity curve generator* for space-based gravitational wave observatories maintained by S. L. Larson. We would like to thank the 2004 Santa Fe Cosmology Workshop where this work was initiated. This research made use of the NASA Astrophysics Data System. SMK was partially supported by Los Alamos National Laboratory (under DOE contract W-7405-ENG-36). ARZ is funded by The Kavli Institute for Cosmological Physics at The University of Chicago and The National Science Foundation through grant No. NSF PHY 0114422.

REFERENCES

- Abel, T., Bryan, G., & Norman, M. 2000, ApJ, 540, 39
 Adams, F. C., Graff, D. S., Mbonye, M., & Richstone, D. O. 2003, ApJ, 591, 125
 Adams, F. C., Graff, D. S., & Richstone, D. O. 2001, ApJ, 551, L31
 Armitage, P. J. & Natarajan, P. 2002, ApJ, 567, L9
 Barafee, I., Heger, A., & Woosley, S. E. 2001, ApJ, 550, 890
 Begelman, M. C., Blandford, R. D., & Rees, M. J. 1980, Nature, 287, 307
 Bond, J. R., Cole, S., Efstathiou, G., & Kaiser, N. 1991, ApJ, 379, 440
 Brandt, S. R. & Seidel, E. 1995, Phys. Rev. D, 52, 870
 Bromm, V., Coppi, P., & Larson, R. B. 2001, ApJ, 527, L5
 Bromm, V. & Loeb, A. 2003, ApJ, 596, 34
 Bullock, J. S., Dekel, A., Kolatt, T. S., Kravtsov, A. V., Klypin, A. A., Porciani, C., & Primack, J. R. 2001, Astrophys.J., 555, 240 (B01)
 Buonanno, A., Sigl, G., Raffelt, G. G., Janka, H.-T., & Müller, E. 2005, PRD, Submitted (astro-ph/0412277)
 Chandrasekhar, S. 1943, ApJ, 97, 255

- Chen, D. N., Jing, Y. P., & Yoshikaw, K. 2003, *ApJ*, 597, 35
- Cornish, N. J. 2003
- Cornish, N. J. & Larson, S. L. 2001, *Class. Quant. Grav.*, 18, 3473
- Dekel, A. & Birnboim, Y. 2004, Submitted (astro-ph/0412300)
- Detweiler, S. 1979, In *Sources of Gravitational Radiation* (Cambridge: Cambridge University Press, 1979, Smarr, L. L., ed.)
- Di Matteo, T., Springel, V., & Hernquist, L. 2005, *Nature*, 433, 604
- Ebisuzaki, T., Makino, J., Tsuru, T., Funato, Y., Portegies, Z. S., Hut, P., McMillan, S., Matsushita, S., Matsumoto, H., & Kawabe, R. 2001, *ApJ*, 552, L19
- Echeverria, F. 1989, *Phys. Rev.*, D40, 3194
- Eisenstein, D. J. & Loeb, A. 1995, *ApJ*, 443, 11
- Enoki, M., Inoue, K. T., Nagashima, M., & Sugiyama, N. 2004, *ApJ*, 615, 19
- Enoki, M., Nagashima, M., & Gouda, N. 2003, *PASJ*, 55, 133
- Farmer, A. J. & Phinney, E. S. 2003, *MNRAS*, 346, 1197
- Favata, M., Hughes, S. A., & Holz, D. E. 2004, *ApJL*, 607, L5
- Ferrarese, L. 2002, *ApJ*, 578, 90
- Ferrarese, L. & Ford, H. 2005, *Space Science Reviews*, 116, 523
- Ferrarese, L. & Merritt, D. 2000, *ApJ*, 539, L9
- Fitchett, M. J. 1983, *MNRAS*, 203, 1049
- Flanagan, E. E. & Hughes, S. A. 1998a, *Phys. Rev. D*, 57, 4535 (FH98)
- . 1998b, *Phys. Rev. D*, 57, 4566
- Fryer, C. L., Holz, D. E., & Hughes, S. A. 2002, *ApJ*, 565, 430
- Fryer, C. L., Woosley, S. E., & Heger, A. 2001, *ApJ*, 550, 372
- Gebhardt, K. et al. 2000, *ApJ*, 539, L13
- Gnedin, O. Y. 2001, *Class. Quant. Grav.*, 18, 3983
- Gould, A. & Rix, H. 2000, *ApJ*, 532, L29
- Granato, G. L. et al. 2001, *MNRAS*, 324, 757
- Haehnelt, M. G. 1994, *MNRAS*, 269, 199
- Haehnelt, M. G., Natarajan, P., & Rees, M. J. 1998, *MNRAS*, 300, 827
- Haehnelt, M. G. & Rees, M. J. 1993, *MNRAS*, 263, 168
- Haiman, Z. & Menou, K. 2000, *ApJ*, 531, 42
- Hatziminaoglou, E., Mathez, G., Solanes, J.-M., Manrique, A., & Salvador-Sole, E. 2003, *MNRAS*, 343, 692
- Heger, A. & Woosley, S. E. 2002, *ApJ*, 567, 532
- Hills, J. G. & Fullerton, L. W. 1980, *Astron. J.*, 85, 1281
- Hills, D. & Bender, P. L. 1995, *ApJ*, 445, L7
- Hogan, C. J. 2000, *Phys. Rev. Lett.*, 85, 2044
- Hughes, S. 2002, *MNRAS*, 331, 805
- Hughes, S. A. & Blandford, R. D. 2003, *ApJ*, 585, L101
- Islam, R. R., Taylor, J. E., & Silk, J. 2004a, *MNRAS*, 354, 427
- . 2004b, *MNRAS*, 354, 443
- . 2004c, *MNRAS*, 354, 629
- Jackson, J. D. 1975, *Classical Electrodynamics* (92/12/31, New York: Wiley, 1975, 2nd ed.)
- Kawaguchi, T., Aoki, K., Ohta, K., & Collin, S. 2004, *A&A*, 420, L23
- Kazantzidis, S., Mayer, L., Colpi, M., Madau, P., Debattista, V., Moore, B., Wadsley, J., Stadel, J., & Quinn, T. 2004, *ApJ*, 623, L67
- Klypin, A., Zhao, H., & Somerville, R. S. 2002, *ApJ*, 573, 597
- Kormendy, J. & Richstone, D. 1995, *ARA&A*, 33, 581
- Koushiappas, S. M., Bullock, J. S., & Dekel, A. 2004, *MNRAS*, 354, 292 (KBD)
- Koushiappas, S. M. & Zentner, A. R. 2005, In preparation
- Lacey, C. & Cole, S. 1993, *MNRAS*, 262, 627
- Larson, S. L., Hiscock, W. A., & Hellings, R. W. 2001, *PRD*, 62, 062001
- Lee, H. M. 1995, *MNRAS*, 272, 605
- Lin, D. N. C. & Pringle, J. E. 1987, *MNRAS*, 225, 607
- Loeb, A. & Rasio, F. A. 1994, *ApJ*, 432, 52
- Lommen, A. N. 2002, in *Neutron Stars, Pulsars, and Supernova Remnants*, 114
- Madau, P. & Rees, M. J. 2001, *ApJ*, 551, L27 (MR01)
- Magorrian, J. et al. 1998, *AJ*, 115, 2285
- Matsubayashi, T., Shinkai, H., & T., E. 2004, *ApJ*, 614, 864
- Menou, K., Haiman, Z., & Narayanan, V. K. 2001, *ApJ*, 558, 535
- Merritt, D. & Ferrarese, L. 2001a, *MNRAS*, 320, L30
- . 2001b, *ApJ*, 547, 140
- Merritt, D. & Milosavljevic, M. 2004, To appear in *Living Reviews of Relativity* (astro-ph/0410364)
- Milosavljevic, M. & Merritt, D. 2001, *ApJ*, 563, 34
- Miralda-Escudé, J. & Kollmeier, J. A. 2003, *ApJ*, Submitted (astro-ph/0310717)
- Misner, C. W., Thorne, K. S., & Wheeler, J. A. 1973, *Gravitation* (San Francisco: W. H. Freeman & Co.)
- Murray, N., Quataert, E., & Thompson, T. A. 2005, *ApJ*, 618, 569
- Navarro, J. F., Frenk, C. S., & White, S. D. M. 1997, *ApJ*, 490, 493 (NFW)
- Nelemans, G., Yungelson, L. R., & Portegies-Zwart, S. F. 2001, *A&A*, 375, 890
- Page, L., Nolta, M. R., Barnes, C., Bennett, C. L., Halpern, M., Hinshaw, G., Jarosik, N., Kogut, A., Limon, M., Meyer, S. S., Peiris, H. V., Spergel, D. N., Tucker, G. S., Wollack, E., & Wright, E. L. 2003, *ApJS*, 148, 233
- Pizzoloto, F. & Soker, N. 2004, *MNRAS*, Submitted (astro-ph/0407042)
- Quinlan, G. D. 1996, *NewA*, 1, 35
- Quinlan, G. D. & Shapiro, S. L. 1990, *ApJ*, 356, 483
- Rhook, K. J. & Wyithe, J. S. B. 2005, *MNRAS*, Submitted (astro-ph/0503210)
- Salucci, P., Szuszkiewicz, E., Monaco, P., & Danese, L. 1999, *MNRAS*, 307, 637
- Sazonov, S. Y., Ostriker, J. P., Ciotti, L., & Sunyaev, R. A. 2004, *MNRAS*, Submitted (astro-ph/0411086)
- Schneider, R., Ferrara, A., Ciardi, B., Ferrari, V., & Matarrese, S. 2000, *MNRAS*, 317, 385
- Sesana, A., Haardt, F., Madau, P., & Volonteri, M. 2004a, *ApJ*, 611, 623
- . 2004b, *ApJ*, 623, 23
- Seto, N., Kawamura, S., & Nakamura, T. 2001, *PRL*, 87, 221103
- Shaerer, D. 2002, *A&A*, 382, 28
- Shapiro, S. L. & Shibata, M. 2002, *ApJ*, 577, 904
- Shapiro, S. L. & Teukolsky, S. A. 1983, *Black holes, white dwarfs and neutron stars* (Wiley)
- Sheth, R. K. & Tormen, G. 1999, *MNRAS*, 308, 119
- Smarr, L. L. 1979, In *Sources of Gravitational Radiation* (Cambridge: Cambridge University Press, 1979, Smarr, L. L., ed.)
- Somerville, R. S. & Kolatt, T. S. 1999, *MNRAS*, 305, 1
- Spergel, D. N., Verde, L., Peiris, H. V., Komatsu, E., Nolta, M. R., Bennett, C. L., Halpern, M., Hinshaw, G., Jarosik, N., Kogut, A., Limon, M., Meyer, S. S., Page, L., Tucker, G. S., Weiland, J. L., Wollack, E., & Wright, E. L. 2003, *ApJS*, 148, 175
- Sperhake, U., Kelly, B., Laguna, P., Smith, K. L., & Schnetter, E. 2005, *Phys. Rev. D*, 71, 123042

- Springel, V., Di Matteo, T., & Hernquist, L. 2004, MNRAS, Submitted (astro-ph/0411108)
- Steed, A. & Weinberg, D. H. 2003, ApJSubmitted (astro-ph/0311312)
- Tegmark, M., Silk, J., Rees, M. J., Blanchard, A., Abel, T., & Palla, F. 1997, ApJ, 474, 1
- Tegmark et al., M. 2004, Phys. Rev. D, 69, 103501
- Thorne, K. S. 1980, Rev. Mod. Phys., 52, 299
- Thorne, K. S. 1987, in Three Hundred Years of Gravitation, 330
- Thorne, K. S. 1995, in Particle and Nuclear Astrophysics and Cosmology in the Next Millenium: Proc. 1994 Snowmass Summer Study, 109
- Thorne, K. S. 1996, in Compact Stars In Binaries, 151
- Thorne, K. S. & Braginsky, V. B. 1976, ApJ, 204, L1
- Tremaine, S. et al. 2002, ApJ, 574, 740
- Turner, M. S. 1997, PRD, 55, 435
- van den Bosch, F. C., Abel, T., Croft, R. A. C., Hernquist, L., & White, S. D. M. 2002, ApJ, 576, 21
- Volonteri, M., Haardt, F., & Madau, P. 2003, ApJ, 582, 559
- Volonteri, M., Madau, P., Quataert, E., & Rees, M. J. 2005, Astrophys. J., 620, 69
- White, S. D. M. & Rees, M. J. 1978, MNRAS, 183, 341
- Wyithe, J. S. & Loeb, A. 2003, ApJ, 590, 691
- Yu, Q. 2002, MNRAS, 331, 935
- Zaldarriaga, M., Furlanetto, S. R., & Hernquist, L. 2004, ApJ, 608, 622
- Zentner, A. R., Berlind, A. A., Bullock, J. S., Kravtsov, A. V., & Wechsler, R. H. 2005, ApJ, 624
- Zentner, A. R. & Bullock, J. S. 2003, ApJ, 598, 49